Premenstrual dysphoric disorder (PMDD) is associated with estradiol-dependent aberrations in intracellular calcium homeostasis and the endoplasmic reticulum stress response

by

Howard Li

Submitted in Partial Fulfillment of the Requirements for the M.D. Degree with Honors in a Special Field at Harvard Medical School

February 4, 2019

Area of Concentration: Reproductive Psychiatry, Molecular Biology

Project Advisor: Peter J. Schmidt, MD (primary advisor)
Janet M. Mullington, PhD (local advisor)

Author's Prior Degrees: B.S. Biochemistry & Cell Biology, UC San Diego, 2013

I have reviewed this thesis. It represents work done by the author under my supervision and guidance.

Faculty Supervisor's Signature

Abstract

Premenstrual Dysphoric Disorder (PMDD) is characterized by debilitating mood symptoms that vary with the menstrual cycle, with evidence suggesting that symptoms are due to an abnormal cellular response to reproductive hormones. However, the molecular and functional correlates of this abnormal hormone response are poorly understood. We performed RNA sequencing (RNAseq) on lymphoblastoid cell lines (LCLs) derived from women with PMDD and asymptomatic controls under untreated (i.e., steroid-free), estradiol-treated (E2), and progesterone-treated (P4) conditions. First, in a module-level analysis of RNAseq data, weighted gene correlation network analysis (WGCNA) identified four modules whose expression showed significant diagnosis x hormone interactions, including one module that was enriched for genes related to neuronal and synaptic function. Enrichment analysis of module hub genes underlying these neuronal enrichment signals revealed multiple pathways related to intracellular calcium dynamics. Next, in a gene-level analysis, a generalized linear model was fitted to RNAseq data and identified 1522 genes differentially responsive to E2 (E2-DRGs) and 480 differentially responsive to P4 (P4-DRGs). Analysis of top E2-DRGs revealed several genes (NUCB1, GCC2, GOLGB1) that were members of a physically interacting network involved in endoplasmic reticulum (ER)-Golgi body function. Independent qPCR validation reproduced a significant diagnosis x E2 interaction ($F(1, 24) = 7.008$, $p = 0.0141$) in NUCB1, a regulator of intracellular calcium and the ER stress response. Finally, we used a thapsigargin (Tg) challenge assay to test whether E2 induces differences in calcium homeostasis and the ER stress response in PMDD, measured by the spliced-to-unspliced XBP1 ratio. Upon Tg treatment, PMDD LCLs had a 27% decreased XBP1 splicing response compared to controls, and pre-treatment with E2 resulted in a statistically significant 38% decreased response ($p = 0.005$), with a significant diagnosis x treatment interaction ($F(3,33) = 3.508$, $P = 0.0259$). Our results suggest that hormone-dependent aberrations in intracellular calcium handling and the ER stress response may contribute to the pathophysiology of PMDD.

Table of Contents

Glossary of abbreviations

PMDD – Premenstrual Dysphoric Disorder
HPG – Hypothalamic-pituitary-gonadal [axis]
LCL – Lymphoblastoid cell line
EBV – Epstein Barr Virus
RNAseq – RNA sequencing
E2 – Estradiol (17β-Estradiol)
P4 – Progesterone (Pregn-4-ene-3,20-dione)
ESC/E(Z) – Extra Sex Combs/Enhancer of Zeste [complex]
H3K27 – Histone H3 lysine 27

RPMI – Roswell Park Memorial Institute [medium]
KOSR – Knockout serum replacement
DMSO – Dimethyl sulfoxide
Tg – Thapsigargin

CASAVA – Consensus Assessment of Sequence And VAriation
SCARF – Solexa compact ASCII read format
WGCNA – Weighted Gene Correlation Network Analysis
GSEA – Gene Set Enrichment Analysis
LEA – Leading Edge Analysis
DRG – Differentially regulated gene
FDR – False Discovery Rate
GO – Gene Ontology
ENCODE – Encyclopedia of DNA Elements
KEGG – Kyoto Encyclopedia of Genes and Genomes
TMM – Trimmed Mean of M-values
ANOVA – Analysis of Variance

NUCB1 – Nucleobindin 1
GCC2 – GRIP And Coiled-Coil Domain-Containing Protein 2
GOLGB1 – Golgin subfamily B member 1
DHCR7 – 7-dehydrocholesterol reductase
PPP2R5D – Protein phosphatase 2 regulatory subunit B'delta
TRPM7 – Transient Receptor Potential Cation Channel Subfamily M Member 7
XBP1 – X-box binding protein 1
s/u XBP1 – Spliced-to-unspliced XBP1 [ratio]

Introduction

Clinical characterization of PMDD

Premenstrual Dysphoric Disorder (PMDD) is a mood disorder characterized by debilitating mood symptoms that vary with the menstrual cycle. As a severe form of Premenstrual Syndrome (PMS), symptoms of PMDD include a combination of mood, behavioral, and physical symptoms. Cardinal mood symptoms are irritability (most common), emotional lability, anxiety, and depression. Other symptoms including anhedonia, fatigue, social withdrawal, appetite and sleep disturbance are also common. Mood and behavioral symptoms are frequently accompanied by at least one physical symptom: abdominal bloating (most common), breast tenderness, swelling, headaches, and muscle aches.[1,2] Importantly, symptoms characteristically occur solely during the luteal phase after ovulation and remit shortly after menses; confirming the cyclicity of symptoms through prospective tracking across at least two consecutive menstrual cycles is critical in establishing a diagnosis of PMDD.[1,3]

PMDD is common and highly morbid. While conservative estimates suggest a prevalence of 3-8% of reproductive-age women,[1,4] this figure is widely thought to underestimate the true prevalence of PMDD due to a variety of reasons: the difficulty of confirming a diagnosis of PMDD in the clinical setting, the misdiagnosis of PMDD for other psychiatric conditions (particularly bipolar disorder), and certainly, a cultural bias – reflected in both patient and provider attitudes – to minimize the severity, significance, and validity of women's mood symptoms.[5,6] Prior to the recent recognition of PMDD as a distinct clinical entity, affected women sought treatment from an average of 3.75 different physicians before being diagnosed with a premenstrual mood disorder.[7] Anecdotal evidence from women with PMDD today suggests that they struggle similarly to reach a diagnosis, though this has not been specifically studied.

In the last two decades, however, there has been a growing awareness among providers to take premenstrual mood symptoms more seriously – a trend largely fueled by studies documenting the true personal, social, and economic burden of disease inflicted by PMDD. While symptoms are intermittent and resolve following the onset of menses, they recur monthly and last an average of 6 days per month for the majority of a woman's reproductive years, totaling nearly 3000 days of severe symptoms over the lifespan. Studies estimating the impact of PMDD on disability-adjusted life-years (DALY) suggests PMDD causes a burden of 3.8 DALYs for each afflicted woman, translating to a total burden of 14,492,465 DALYs in the U.S. alone.[4] Another study comparing health-related quality of life (HRQoL) measures in women with PMDD with those of the general U.S. female population found that the HRQoL burden of PMDD

was comparable to or greater than the HRQoL burdens of chronic back pain, type 2 diabetes, hypertension, and rheumatoid arthritis.[8] As PMDD affects women during reproductive years – a time when women often have school, family, and career responsibilities – the economic impact of PMDD is also significant. Women with PMS/PMDD experience double the amount of health-related work absenteeism compared with women without PMS/PMDD, and experience a high degree of impairment in social activities and personal relationships.[9] While direct costs due to health care visits due to PMS/PMDD are estimated to be $59 per year, indirect costs due to missed work and decreased work productivity amount to at least $4333 per year.[10] Most strikingly, PMDD is associated with a 15% lifetime risk of attempted suicide, compared to about 4-5% in the general population.[11,12]

While PMDD was previously a diagnosis outlined only in an appendix of the DSM-IV, its codification as a full diagnostic category in the DSM-5 is a relatively recent development, reflecting maturing evidence suggesting that PMDD is both etiologically and clinically distinct from other mood disorders.[13]

Abnormal hormone response in the etiology of PMDD

While the etiology and pathophysiology of PMDD is poorly understood, several studies have established a modern understanding of PMDD as a disease of abnormal neuropsychiatric response to ovarian steroids such as estrogens and progesterone. As mentioned, symptoms characteristically occur solely during the luteal phase shortly after ovulation, and remits shortly after menses. This clinical pattern of symptom variation with the menstrual cycle suggested a role for reproductive hormones such as estrogens and progesterone in triggering symptoms.

While a few small studies have reported a difference in serum levels of endocrine factors (estrogens, progesterone, cortisol, insulin) between PMDD and healthy controls,[14–17] the overall consensus of large studies is that PMDD is not associated with any differences in reproductive hormones in PMDD, and that HPG axis activity, hormone levels, ovulatory function, and menstrual cycling are normal in PMDD patients.[18–20] Alternatively, it was posited that PMDD is not a disease cause by a pathological aberration in quantitative hormone levels, but rather, an abnormal behavioral or cellular response to the normal, physiologic fluctuations of reproductive hormones that occur during the menstrual cycle. This putative mechanism was supported by the clinical observation PMS/PMDD symptoms appear to improve with HPG-suppressing agents such as leuprolide and anti-estrogens such as danazol, and localizes the etiology of PMDD at a process at or downstream from the receptor-hormone interaction. Most definitively, in 1998, Schmidt et al demonstrated through clinical hormone manipulations that physiologic fluctuations

in estradiol or progesterone were both causal factors of mood symptoms in women with PMDD. The study recruited women meeting diagnostic criteria for PMDD and found that women would not only experience symptom remission with pharmacologic suppression of the hypothalamic-pituitary-gonadal (HPG) axis with leuprolide, but also that mood symptoms could be reproduced when physiologic levels of either estradiol (E2) or progesterone (P4) were added back in a double-blind crossover design. This effect was not seen in healthy controls, which showed no change in mood symptoms with leuprolide HPG suppression or hormone add-back.[21] It was further shown that while fluctuating levels of estradiol and progesterone trigger behavioral symptoms in PMDD, continuous, stable levels do not.[22] Since then, therapies targeting the HPG-axis have been shown to be an efficacious method of treating PMDD, and current treatment guidelines consider oral contraceptives (OCPs) an acceptable first-line treatment for patients with suspected PMDD, along with selective serotonin reuptake inhibitors (SSRIs).[1]

In light of the finding that normal, physiologic fluctuations in ovarian steroids were causal factors in the pathogenesis of PMDD, multiple studies have attempted to characterize the pathophysiology of abnormal response to ovarian hormones in PMDD. Neuroimaging studies have found that women with PMDD demonstrate hormone-induced differences in neurocircuitry and cognition, including emotional processing, corticolimbic control, and working memory.[23–27] For example, Gingell et al conducted a functional MRI study on women with PMDD and healthy controls, and found that, specifically in the luteal phase, women with PMDD showed increased reactivity in the amygdala and insula and decreased reactivity in the anterior cingulate cortex in response to aversive social stimuli, compared to healthy controls – a finding that perhaps correlates clinically with irritability, emotional reactivity, and impaired social functioning in PMDD patients, and suggests that these symptoms may be due to altered corticolimbic processing in the luteal phase.[25] A larger, more recent study also found that women with PMDD demonstrated decreased activation of the dorsolateral prefrontal cortex in the luteal phase during a validated emotional regulation-task.[28] In the last decade, functional neuroimaging studies have provided increasing support for hormone-dependent, functional differences in brain function, and this continues to be an area of active study, including as a tool to investigate the effects of potential hormonal therapies.[29,30]

Evidence for the genetic and molecular basis of PMDD

There is limited but growing evidence that these behavioral, cognitive, and functional neuroanatomical findings may be underpinned by genetic and molecular factors. A 1991 prospective study of 20 mother-daughter dyads suggested the earliest evidence of heritability of

PMS symptoms, with daughters being more likely to experience premenstrual symptoms if their mothers also experienced symptoms.[31] A twin study of 827 pairs of female same-sex twins estimated a 35% heritability of premenstrual symptoms,[32] and a larger, longitudinal study of 1,312 pairs of female same-sex twins found a time-stable heritability of premenstrual symptoms at 56%.[33] While one analysis of a PMDD case-control cohort identified several risk-conferring polymorphisms of ESR1, which codes for estrogen receptor alpha,[34] the search for genetic variants associated with PMDD is an active area of study.

In recent years, the search for causal molecular pathways in the pathophysiology of PMDD has yielded several promising leads. Progesterone metabolites are known to have neuroactive, mood-modulating properties, and one endogenous progesterone metabolite, allopregnanolone, has been shown to be a potent modulator of GABAergic pathways of the brain.[35,36] Preliminary evidence suggests that while allopregnanolone, as a positive allosteric modulator of the GABA-A receptor, characteristically has an anxiolytic effect, in women with PMDD, allopregnanolone may have a paradoxical, anxiogenic effect.[37,38] Brain-derived neurotrophic factor (BDNF) is also a molecule of interest. BDNF is expressed abundantly in the brain and involved in multiple critical functions, including learning, memory, and affective regulation. Genetic variants of BDNF, particularly the Val66Met polymorphism, have been associated with neuropsychiatric disorders including depression, anxiety, bipolar disorder, and schizophrenia.[39] Neuroimaging studies have also found that the BDNF Val66Met allele modulates that effect of luteal phase hormones on the brain in both healthy women and women with PMDD.[40,41] When the BDNF Val66Met allele was introduced into a mouse model, recombinant mice exhibited estradiol-dependent behavior changes that mimicked those of PMDD that were not seen in wild-type nice.[42] There is also preliminary, though inconsistent, evidence of significant differences in luteal phase serum concentrations of BDNF levels in women with PMDD compared to controls.[43,44] Finally, other studies have implicated neuroimmune interactions as potentially causal in the pathophysiology of PMDD. It is known that the luteal phase hormones, particularly progesterone, are associated with an increase in proinflammatory signals such as interleukin-6, TNF-α, and C-reactive protein,[45,46] and these inflammatory mediators may be present in elevated levels in women with PMS/PMDD.[47] In light of emerging evidence implicating inflammation and neuroimmune interactions in the pathophysiology of mood disorders such as major depression,[48,49] the role of inflammation in PMDD is one hypothesis that is also currently being pursued.

Lymphoblastoid cell lines and the cellular basis of PMDD

If PMDD is genetically heritable, with certain genes, proteins, and molecular pathways plausibly contributing to its pathophysiology, could PMDD be associated with intrinsic differences at the cellular level? In studying cellular differences in PMDD, patient-derived lymphoblastoid cell lines (LCLs) may be a convenient in-vitro model. LCLs are culturable cell lines derived from the treatment of mononuclear cells with infection with Epstein-Barr Virus (EBV), which specifically targets B-lymphocytes through a viral CD21 receptor and generates infected B cells with unlimited growth capacity in-vitro, and presumably, continue to reflect certain functional characteristics dictated by the genomes of patients from whom they were derived.[50,51] Acknowledging important limitations, LCLs can be easily derived from peripheral blood samples, cultured in the laboratory, and assayed for biochemical, molecular, or functional differences under controlled conditions, including in-vitro hormone exposure.[52–54] In this way, LCL models have been used to uncover relevant biology in a number of clinically-relevant scenarios, including genetic diseases,[55–57] neuropsychiatric conditions,[58–63] and personalized medicine.[51,64,65]

In 2017, Dubey et al published the results of an LCL-based study of PMDD. As the first study to examine cell-level differences in PMDD, Dubey et al used RNA sequencing (RNAseq) to conduct a transcriptomic analysis of LCLs derived from 10 women with a diagnosis of PMDD confirmed by both prospective symptom tracking and clinical hormone manipulation, and 9 women who served as healthy controls. Their analysis discovered that the ESC/E(Z) complex, a complex of 13 genes involved in epigenetic silencing via H3K27 methylation and also implicated in behavior and stress, is differentially expressed in PMDD.[66] Of note, the ESC/E(Z) complex is involved in modulating the transcriptional response to steroid hormones, particularly estrogens – a relationship well-defined by studies detailing the role of ESC/E(Z) and its critical methyltransferase component EZH2 in estrogen-responsive cancers.[67–70] This finding provided the first evidence for an intrinsic cellular difference in women with PMDD, and opens questions for further investigation, especially in light of the ESC/E(Z) complex's role as a potential epigenetic regulator of downstream functions. However, while PMDD has been hypothesized to be a disease of abnormal response to hormone, the finding of altered ESC/E(Z) expression was discovered when comparing PMDD and control LCLs primarily in the baseline, untreated (steroid-free) condition. Indeed, while baseline differences in ESC/E(Z) complex expression could serve as a potential substrate for the abnormal response to hormone hypothesized to be central to the pathophysiology of PMDD, the molecular and functional correlates of a differential

hormone response (including the transcriptional consequences of altered ESC/E(Z) complex expression), have not been well-described.

In this study, we first explore the transcriptomic basis of a differential hormone response in PMDD using two approaches: a module-level analysis to identify differentially regulated gene modules and their associated functions, and a gene-level analysis using linear modeling of RNAseq data in EdgeR to identify differentially regulated genes. Informed by the results of our module-level and gene-level transcriptomic analyses, we then designed an in-vitro assay to test whether there was a hormone-dependent functional difference in intracellular calcium homeostasis between PMDD and control LCLs.

Methods

Participants

Women were recruited for this study as previously described.[66] Briefly, women were aged 18-48 years, had regular menstrual cycles (21-35 days in duration), and were not medically ill, taking medications, or pregnant at the time of recruitment. Women with PMDD were self-referred in response to newspaper advertisement or referred by their physician, and DSM-IV criteria for PMDD were prospectively confirmed through daily self-administered symptom ratings over three consecutive menstrual cycles.[71] Women were also assessed through clinical interview and a self-report questionnaire to confirm that diagnostic criteria were met. In addition to the DSM-IV diagnostic criteria, each woman had average self-ratings of negative symptoms (irritability, depression, anxiety, and mood lability) that were at least 30% greater in the 7 days before menses, compared to the 7 days after the end of menses, relative to the range of the scale employed by each woman. Women whose self-ratings showed significant mood symptoms outside of the luteal phase were excluded.

Women without PMDD (asymptomatic controls) were also recruited, and the absence of premenstrual symptoms was confirmed using the same daily rating scales over 2 months. Women contributing samples for LCL generation for RNAseq analysis all underwent a trial of gonadal suppression with leuprolide and hormone add-back. Women included in the PMDD group for RNAseq analysis experienced symptom remission by leuprolide and symptom recurrence with either estradiol or progesterone addback, using defined criteria as previously described.[21] Women included in the control group were asymptomatic throughout the entire trial of Lupron and add-back. A completely independent cohort of women contributing samples for experimental validation was also recruited using the same criteria defined above, but did not

undergo hormone manipulation trials. Demographics of women contributing samples to each study component are summarized in **Supplemental Table S1**.

The study protocol was approved by the Combined NeuroScience IRB within the NIMH Intramural Research Program. All women provided written informed consent and received payment for participation according to NIH intramural guidelines.

Cell culturing, hormone treatments, and RNA sequencing

Briefly, LCLs were derived from mononuclear cells isolated from peripheral blood samples of women using the method outlined by Oh et al.[50] Once LCLs were established, they were seeded at 2×10^5 cells/mL in phenol-free RPMI 1640 media (Gibco, cat. no. 11835-055) with 15% knock out serum replacement (KOSR) (Gibco, cat. no. 10828-028), 2% glutamine (200 mM), and 1% gentamicin (5 mg/ml) and cultured for 3-5 days at 37°C with 5% CO2 before undergoing treatment with estradiol (100 nM, Sigma-Aldrich, cat. no. E2758-5G) or progesterone (100 nM, Sigma-Aldrich, cat. no. P8783-25 G) for 24 hours, or no treatment. Full details are described in Dubey et al.[66] After the 24h treatment period, cells were harvested for RNAseq library preparation.

Total RNA from cell pellets was isolated using the TRIzol extraction method (Life Technologies, cat. no. 15596018), treated with DNase (Qiagen, cat. no. 79254), and further purified using the RNeasy MinElute Cleanup kit (Qiagen, cat. no. 74204). RNA quality was analyzed on the Agilent 2100 Bioanalyzer, and total RNA was used to prepare cDNA libraries using the Ambion RNAseq library construction kit (Invitrogen, cat. 4454073). Libraries were sequenced on the Illumina Genome Analyzer IIx system. Raw RNAseq reads in SCARF format from Illumina pipeline CASAVA_v1.8.1 were exported as FASTQ reads for further analysis. FASTQ reads were aligned to the UCSC hg19 reference genome using TopHat2 using a read segment length of 25, mismatch and gap thresholds of 2, insertion and deletion thresholds of 3, and minimum splice anchor length of 8.[72] The featureCounts tool in the Subread package was used to generate genewise counts from mapped bam files.[73] Counts were converted to CPM and RPKM values using an in-house script.

Schematic representation of subsequent analysis of RNAseq data is summarized in **Figure 1.**

Module-level analysis: WGCNA, GSEA, and Enrichr

Weighted Gene Correlation Network Analysis (WGCNA) was conducted using the WGCNA R package v.1.66.[74] WGCNA uses coexpression patterns between genes across a set

of RNAseq samples to discover, in an unsupervised manner, clusters of co-regulated genes ("modules").

Modules were generated from CPM values of 46 input samples (**Supplemental Table S2**) using an unsigned correlation measure, soft thresholding power of 4, minimum module size of 30, and a merge cut height of 0.25. Discovered modules are assigned colors (e.g. Red, Green, DarkOrange, etc.) as arbitrary, non-ordinal identifiers. To identify differentially responsive modules, the values of module eigengenes were extracted from each module across all input samples. An eigengene is defined as the first principle component of genes within a given module, and used as a robust measure of overall expression activity of that module. Two-way ANOVA analysis was performed on module eigengenes, and modules with eignegenes showing a significant diagnosis x hormone interaction ($p < 0.05$) were considered to be differentially responsive.

Functional analysis of module genes was conducted using the Gene Set Enrichment Analysis (GSEA)[75] and Enrichr tools.[76,77] In GSEA, pre-ranked module genes were analyzed against the C5 Gene Ontology gene sets downloaded from MSigDB 6.2 Collections[78–80] with 1000 permutations. Importantly, module genes were pre-ranked by the WGCNA intramodular connectivity metric, in order to place greater weight on high connectivity hub genes during enrichment analysis. A less stringent threshold of an FDR-corrected q-value < 0.25 was chosen for significantly enriched gene sets for the purposes of data exploration, per published recommendations.[75]

As secondary analysis, we wanted to identify the specific cellular pathways and functions represented by the broad functional terms identified in GSEA results. To do this, we used the Leading Edge Analysis (LEA) function within the GSEA package, which identifies the subset of high-ranked genes within an input gene set that contributes most to an enrichment signal. LEA subsets were identified for each of the top 20 enrichment signals identified by GSEA, and the union of these 20 LEA subsets was used for further analysis in Enrichr. In Enrichr, an unweighted list of LEA genes was queried for analysis against four databases: 1. ENCODE and ChEA Consensus TFs from ChIP-X,[81–83] 2. NIH Roadmap Epigenomics Histone Modification ChIP-seq data set,[84,85] 3. KEGG's cell signaling pathways (2016),[86] and GO terms for Biological Processes, Molecular Function, and Cellular Component (2018).[78,79]

Gene-level analysis: EdgeR, GeneMANIA, and qPCR

We used generalized linear modeling of RNAseq data within EdgeR[87] to identify individual genes that were differentially regulated by either E2 (E2-DRGs) or P4 (P4-DRGs).

Each set of paired RNAseq samples (untreated and E2-treated, and untreated and P4-treated) was used to fit a separate model. Paired RNAseq samples with TMM-normalized counts and tagwise dispersion estimation were fitted to a quasi-likelihood negative binomial generalized log-linear model in which the factors of subject (cell line) and treatment (untreated vs. hormone-treated) were both nested under diagnosis (control vs. PMDD).[88] Genewise F-tests were then performed to identify genes showing significant diagnosis x hormone interactions (nominal $P < 0.05$), yielding a list of genes differentially responsive to E2 (E2-DRGs) or to P4 (P4-DRGs).

Visualization of gene interaction networks of identified DRGs was performed in GeneMANIA, a web-based network visualization tool that accepts an unranked list of genes and generates a weighted interaction network based on published databases of co-expression, physical interactions, co-localization, shared pathways, genetic interactions, and shared protein domains. The GeneMANIA tool was accessed for network visualization of select E2-DRGs in January 2019.

qPCR validation of select differentially-regulated genes were conducted using TaqMan gene expression assays (Applied Biosystems). Total RNA was extracted as described above, and ~1 ug total RNA was used for cDNA synthesis, conducted at 20 uL reaction volumes using the Applied Biosystems High-Capacity cDNA Reverse Transcription Kit (cat. no. 4368814). TaqMan qRT-PCR assays were then conducted using the following probes: ACTB: Hs01060665_g1, NUCB1: Hs00939167_m1, DHCR7: Hs01023087_m1, GOLGB1: Hs00189566_m1, PPP2R5D: Hs00605059_m1 (cat. no. 4448490, 4331182). qPCR reactions were conducted in triplicate at 10 uL reaction volumes on the 7900HT Fast Real-Time PCR System (Applied Biosystems) with the following cycling conditions: polymerase activation at 95 °C for 10 min, and amplification at 95 °C for 15 s and 60 °C for 1 min for 40 cycles. Relative expression levels were calculated using the ΔΔCT method using beta-actin (ACTB) as the reference gene.[89]

Thapsigargin challenge assays

LCLs were seeded at 2×10^5 cells/mL in phenol-free RPMI with 15% KOSR, 2% glutamine, and 1% gentamicin as above, divided into 5 ml cultures in 6-well plates, and cultured at 37°C, with 5% CO2 at 3-5 days. For E2 pre-treatments, E2 in DMSO was added for a final concentration of 100 nM, and cells were cultured for 20 h. An equivalent amount of DMSO was used as a vehicle control. For Tg treatments, Tg in DMSO was added for a final concentration 0.2 uM Tg, and $CaCl_2$ in water was added for a final concentration of 0.8 uM $CaCl_2$, and cultured for an additional 4 hours before cells were harvested. RNA extraction and cDNA synthesis were

performed as described above. Spliced-to-unspliced XBP1 ratios (s/u XBP1) were quantified via qPCR in triplicate using primers specific for spliced and unspliced XBP1 transcripts as specified by Oslowski et al.[90] Reaction mix consisted to 5 uL SYBR Select Master Mix (2x), 1 uL of each primer (2 uM), 1 uL cDNA template, and 2 uL nuclease-free water for a total reaction volume of 10 uL. The following cycling settings were used: polymerase activation at 95 °C for 10 min, and amplification at 95 °C for 10 s and 58 °C for 30 s for 40 cycles. Relative levels of s/u XBP1 were calculated using the ΔΔCT method.[89]

Statistical analysis

Statistical analyses were performed in GraphPad Prism version 8 (La Jolla, CA) and R version 3.4.1 (Vienna, Austria).[91] Student's T test and Fisher's Exact tests were conducted for demographic variables. Analysis of qPCR data for E2-DRG validation and Tg challenge assays were performed with repeated measures ANOVA with Sidak's multiple comparisons testing in post-hoc analysis.

Results

WGCNA identifies modules associated with abnormal hormone response in PMDD LCLs, including one associated with the ESC/E(Z) complex.

Of 26 362 genes represented by the 46 input RNAseq libraries, 22 242 (84%) were sufficiently expressed for clustering analysis. Of these, 21 746 genes (98%) were clustered into 65 modules, while 496 genes were left unclustered (**Figure 2a**) Four modules had eigengenes with significant diagnosis x hormone interactions (brown, pink, turquoise, and magenta). Of these, the brown, pink, and turquoise modules were also among seven modules that showed a significant main effect of diagnosis. Additionally, 10 modules showed a significant main effect of hormone treatment, including the turquoise module (**Figure 2b, Table 1**).

All of ESC/E(Z) complex genes (EZH2, SUZ12, EED, RBBP4, AEBP2, EZH1, HDAC2, JARID2, MTF2, PHF1, PHF10, RBBP7, SIRT1) were clustered into modules with eigengenes showing significant effects of diagnosis, hormone treatment, and/or the interaction of diagnosis and hormone: Turquoise (6 genes), Blue (2), AntiqueWhite4 (1), Cyan (1), DarkOliveGreen (1), Green (1), SkyBlue2 (1) (**Figure 2c**). Nearly half of ESC/E(Z) genes were assigned to the turquoise module (SIRT1, MTF2, AEBP2, HDAC2, SUZ12, and EED), where they are high-connectivity and high-significance members (**Figure 2d**).

Modules associated with differential hormone response are enriched for genes related to chromatin modeling and RNA processing, MAPK signaling, mitochondrial function, and neuronal processes.

To explore the functions represented by modules associated with significant hormone x diagnosis interactions (brown, pink, turquoise, magenta), modules genes were rank-ordered by intramodular connectivity and analyzed via gene set enrichment analysis (GSEA) for functional enrichment of known Gene Ontology (GO) terms. The turquoise module was enriched for terms relating to chromatin remodeling, proteasome function, and transcriptional processing. The pink module was enriched for terms relating to mitochondrial function. The brown module contained many terms for MAP Kinase and GTPase signaling. Finally, the magenta module was highly enriched for terms relating to neuronal and synaptic function (**Figure 2e**)**.** Complete GSEA results are reported in **Supplemental Table S3**.

Key genes in the neuronally-relevant magenta module represent pathways relating to synaptic transmission and intracellular calcium dynamics.

Leading Edge Analysis (LEA) of top 20 enriched magenta module GO terms yielded a core subset of 88 LEA genes (**Supplemental Table 4**). Enrichr analysis found that magenta LEA genes were enriched for targets of SUZ12 and EZH2 and estrogen receptor ESR1 (**Figure 3a**), and for genes associated with the H3K27me3 histone marker across multiple cell lines (**Figure 3b**). The top enriched KEGG pathways were neuroactive ligand-receptor interaction, the cAMP, Rap1, Ras, and Wnt intracellular signaling pathways, and glutamatergic and dopaminergic synapses (**Figure 3c**). Upon searching for enriched GO terms, we found that – among other functions such as membrane receptor function, synaptic transmission, and G-protein and protein kinase signaling – GO terms relating to intracellular calcium dynamics were frequently enriched, and included terms relating to calcium-dependent synaptic vesicle handling and calcium ion transport (**Figure 3d-f**). Full Enrichr results are reported in **Supplemental Table S5.**

Top E2-DRGs comprise a physically-interacting network involved in ER-Golgi structure and function.

Linear modeling of RNAseq data in EdgeR identified 1522 genes were differentially responsive to E2 (E2-DRGs) and 480 were differentially responsive to P4 (P4-DRGs). Full EdgeR results for E2-DRGs and P4-DRGs are listed in **Supplemental Tables S6-S7**.

We chose to focus on the E2-treated condition in subsequent analysis and experiments for several reasons: 1. The E2-treated condition appeared to be driving the diagnosis x hormone interaction seen in our modules of interest (**Figure 2b**), 2. There were no P4-DRGs with an FDR < 0.25. 3. Hierarchical clustering of RNAseq samples showed strong clustering of E2-treated samples but not P4-treated samples, and stronger segregation between cases and controls within the E2-treated cluster (**Supplemental Figure S1a**), and 4. Modules of interest were more likely to be enriched for E2-DRGs rather than P4-DRGs. Modules most enriched for P4-DRGs were not significantly associated with diagnosis or differential hormone response (**Supplemental Figure S1b**).

The top 10 E2-DRGs identified through differential expression analysis are listed in **Table 2**. Heuristic analysis of these genes identified several that appear to be directly related to intracellular calcium handling, vesicle trafficking, and the ER-Golgi compartment (NUCB1, GCC2, and GOLGB1). Key genes relating to ER-Golgi function and intracellular calcium homeostasis were selected from among the top 10 E2-DRGs and included as inputs for GeneMANIA network visualization: NUCB1, GCC2, and GOLGB1. TRPM7, another significant E2-DRG ($p = 0.008$) that codes for a cation channel responsible for regulated calcium entry into the cytosol, was also included as an input.[92,93] The resulting output revealed a structural network of Golgi-ER-associated genes, with physical interactions comprising 67.6% of the weighted network (**Figure 4a**).

Select genes were chosen for qPCR validation using TaqMan probes in a completely independent replication cohort of 13 cases and 13 controls. Repeated measures ANOVA analysis on NUCB1 qPCR measures revealed a significant main effect of diagnosis ($F(1, 24) = 4.605$, $p = 0.0422$) and a significant interaction of diagnosis and hormone treatment ($F(1, 24) = 7.008$, $p = 0.0141$), and in post-hoc multiple comparisons testing, E2-treated PMDD samples had significantly reduced NUCB1 expression compared to control samples ($p = 0.0030$). qPCR results for DHCR7 did not reveal significant effects of diagnosis, hormone, or their interaction, but in multiple comparisons testing, DHCR7 expression was significantly reduced in E2-treated PMDD samples compared to E2-treated control samples ($p = 0.0395$). No significant results were found in qPCR validation for PPP2R5D or GOLGB1 (**Figure 4b**).

E2 induces differences in intracellular calcium homeostasis and the ER stress response in PMDD LCLs

Since a module-level analysis identified several calcium-related pathways associated with the differentially-responsive, neuronally relevant magenta module, and gene-level

investigation identified and validated NUCB1, a regulator of intracellular calcium, as an E2-DRG, we hypothesized that PMDD LCLs may demonstrate E2-dependent differences in intracellular calcium handling. To test the hypothesis that E2-treatment would induce differences in intracellular calcium homeostasis, we measured the response of LCLs to a thapsigargin (Tg) challenge assay. Tg is a potent inhibitor of the sarco/endoplasmic reticulum Ca^{2+}-ATPase (SERCA) channel, which transports cytosolic calcium ions into the endoplasmic reticulum (ER) and Golgi apparatus, which serve as endosomal calcium storage compartments.[94–96] Inhibition of the SERCA channel with Tg rapidly increases cytosolic calcium levels while also depleting endosomal calcium stores, which in turn, activates calcium channels in the plasma membrane in a mechanism known as store-operated calcium entry (SOCE), further increasing cytosolic calcium.[97,98] One well-studied response to intracellular calcium perturbations is the ER stress response, also known as the unfolded protein response, which rapidly initiates the expression of genes to maintain intracellular calcium homeostasis and support proper protein folding.[99,100] Activation of the ER stress response by Tg is reliably measured of XBP1 splicing by qPCR.[90,101]

In our Tg challenge assay, we tested the effects of Tg and E2-treatment, alone and in combination, on the ER stress response in PMDD and control LCLs (**Figure 5a**). Repeated Measures ANOVA analysis showed a significant main effect of treatment ($F(3,33) = 11.22$, $P < 0.001$), and a significant diagnosis x treatment interaction ($F(3,33) = 3.508$, $P = 0.0259$). The effect of diagnosis was nearly significant ($F(1,11) = 4.25$, $P = 0.0637$). In post-hoc analysis, we find that control LCLs had a 1.7-fold increase in XBP1 splicing from baseline with Tg alone ($p = 0.0085$), and a 2.2-fold increase with Tg preceded by E2 ($p < 0.0001$). In contrast, PMDD LCLs showed a blunted, non-significant increase in XBP1 splicing in both conditions. Comparing PMDD and control LCLs within treatment conditions, the splicing response of PMDD LCLs was 1.36-fold decreased compared to control LCLs in the Tg-only condition ($p = 0.25$), and this difference was accentuated and significant when Tg was preceded by E2, with a 1.62-fold decreased splicing response ($p = 0.005$). E2 alone did not have a significant effect on XBP1 splicing from baseline in either control or PMDD LCLs (**Figure 5b**). Full ANOVA-RM results are reported in **Supplemental Table S8.**

Discussion, Conclusions, and Suggestions for Future Work

Following the gradual recognition of PMDD as a distinct clinical entity characterized by neuropsychiatric vulnerability to physiologic fluctuations of ovarian steroids during the menstrual cycle, multiple clinical and neuroimaging studies have defined PMDD as a disease of abnormal behavioral response to reproductive hormones. While it was recently reported the cells of

women with PMDD exhibit an intrinsic cellular difference in ESC/E(Z) complex expression in the baseline (steroid-free) condition that may serve as a foundation for an abnormal cellular response upon steroid exposure, the transcripts, pathways, and cellular functions that underpin the differential response to hormone in PMDD remain poorly defined. Through co-expression network analysis of LCL transcriptomes, we identified four gene modules whose activity was differentially responsive to hormones in PMDD; one of these modules was highly enriched for genes governing neuronal and synaptic function, and for targets of ESC/E(Z) complex genes EZH2 and SUZ12. Analysis of key genes in this module and of top E2-DRGs (including the validation of calcium-regulating gene NUCB1) suggested a role for altered intercellular calcium handing and the Golgi-endomembrane system. Informed by our transcriptomic analysis, we designed a functional assay to show that, while control LCLs demonstrate a robust and E2-dependent ER stress response (as measured by XBP1 splicing following Tg treatment), both the ER response and its modulation by E2 appear to be blunted in PMDD. Thus, starting from a global analysis of transcriptomic data, this study is the first to demonstrate a hormone-dependent, functional difference in the cells of women with PMDD.

In our analysis of WGCNA modules for diagnosis x hormone interactions, each module identified as differentially responsive to hormone represents a plausible molecular mechanism in the pathophysiology of PMDD. The turquoise module was enriched for genes relating to chromatin modification (including genes of the ESC/E(Z) complex), proteasome function, and transcriptional processing. The coordinated expression of chromatin modifying genes such as the ESC/E(Z) complex with proteosomal genes within the turquoise module may be one mechanism that explains the previously reported finding that while transcripts of the ESC/E(Z) gene complex were significantly increased in PMDD, protein levels were paradoxically decreased.[66] Indeed, the proteasome has been identified as an important regulator of polycomb-group proteins such as those of the ESC/E(Z) complex, and other chromatin-modifying agents.[102,103] Polyubiquitination and proteolysis have recently been shown to be critical in synaptic development, fidelity, and plasticity,[104–108] and aberrant proteasome function has been implicated in several psychiatric and neurodegenerative disorders.[109–114] Proteasome function is also important for nuclear steroid receptor action, including those of estradiol and progesterone.[115–118] Brown and pink modules were enriched for genes relating to MAP Kinase and GTPase signaling and for genes relating to mitochondrial function, respectively. Both these pathways have been implicated in the molecular pathophysiology of mood disorders, including sex differences.[119–125]

The isolation of the neuronally-relevant magenta module by WGCNA, as well as its identification as a differentially regulated module (i.e. eigengene expression showing a significant diagnosis x hormone interaction), is particularly notable because our RNAseq data was derived from LCLs, a non-neuronal cell line. The ability of peripheral cell lines to model pathophysiologic changes of the brain is controversial and seen as an important limitation to the use of LCLs for studying neuropsychiatric diseases.[52,53] To our knowledge, while multiple studies using LCLs to study psychiatric diseases have identified individual genes of potential neuronal relevance,[58–60,63,126,127] with several others identifying significant modules enriched with non-specific cellular or immunologic processes,[62,128–131] this is first study to isolate a transcriptional module specifically enriched for neuronal functions from LCL transcriptomes – a finding with potentially important implications on the extent to which LCLs may serve as a model of neuropsychiatric disease.

GSEA results of magenta module genes ("Synaptic membrane", "Neuron part", "Axon", etc.), although interesting for their abundance of neuronally-relevant terms, were too broad to inform an actionable hypothesis for investigation in a non-neuronal cell line such as LCLs. Thus, as a secondary analysis to identify more specific, assayable pathways underlying these broad neuronal enrichment signals, we compiled Leading Edge subset genes from the top 20 GSEA enrichment signals to form a union set of 88 LEA genes. Because LEA subsets prioritize high-rank (high-connectivity) genes, this process effectively selects for the neuronally-relevant hub genes of magenta module. In Enrichr analysis, we found that LEA genes of the magenta module were enriched for targets of polycomb complex genes SUZ12 and EZH2, and the estrogen receptor ESR1 – a finding that suggests a relationship between the ESC/E(Z) complex, estrogen response, and transcriptional control of key magenta module genes. The potential role of the ESC/E(Z) complex in the transcriptional control of magenta module genes is reinforced by the finding that magenta LEA genes were also highly enriched for genes associated with the H3K27me3 histone marker across multiple cell lines. This is significant, since the ESC/E(Z) complex is specifically responsible for modification at the H3K27 site,[132,133] and conversely, the only known methyltransferase associated with the H3K27me3 marker is EZH2.[134] One hypothesis that emerges from this analysis that the activity of a set of genes involved in neurotransmission and synaptic function (represented by the magenta module) may be aberrantly regulated by H3K27 epigenetic remodeling (represented by the turquoise module and the ESC/E(Z) complex) in PMDD.

Finally, among several enriched GO terms of high potential relevance to psychiatric disease ("anterograde trans-synaptic signaling," "opioid receptor activity," "ionotropic glutamate

receptor complex"), Enrichr also included multiple GO-terms related to intracellular calcium handling ("calcium ion transmembrane transporter activity," "calcium-dependent phospholipid binding," "cation channel complex," "regulation of calcium ion-dependent exocytosis"). This enrichment of calcium-related GO terms provides notable context for our discovery of NUCB1 as an E2-DRG confirmed with independent validation. NUCB1 is a major calcium-binding protein of the Golgi body, and shown to regulate intracellular calcium uptake and storage in the Golgi lumen.[135,136] Structural analysis of NUCB1 suggests that it acts as a calcium sensor capable of large conformational change upon calcium binding,[137] and indeed in a variety of endocrine tissues, NUCB1 and its homolog NUCB2, are known to govern the calcium-dependent secretory activity of metabolic hormones such as insulin.[138–142] In neurons, NUCB1 is thought to be critical in the monitoring and spatiotemporal regulation of intracellular calcium levels in neurotransmission.[142] Finally, NUCB1 is also a known regulator of the ER stress response, a robust and highly conserved cellular response to unfolded proteins and intracellular calcium perturbations.[143]

NUCB1 appeared as a top E2-DRG in concert with other Golgi body proteins. GCC2 and GOLGB1 were both among the top 10 E2-DRGs identified in linear modeling of RNAseq data, and shown via GeneMANIA visualization to physically interact with NUCB1. GOLGB1 is an integral structural protein in the Golgi body, and responsible for forming cross-bridges between the Golgi cisternae. GCC2 acts as a molecular tether between transport vesicles and the trans-Golgi body, and participates in the targeting of secretory vesicles. Together, these genes suggest that calcium-dependent trafficking of secretory vesicles from the Golgi body, especially in light of enriched magenta module GO terms such as "regulation of calcium ion-dependent exocytosis" and "anterograde trans-synpatic signaling", could be a key disrupted pathway in both neurons and LCLs.

There is emerging evidence for the role of NUCB1 in behavior. Sundarrajan et al showed that NUCB1 expression was modulated by sex steroids estradiol and testosterone, and stimulated anorexia in female goldfish.[144] The homolog NUCB2 is a well-characterized mediator of anorexia and satiety,[145] but has also been found to be a sex-specific regulator of mood and behavior.[146] Circulating levels of NUCB2 was positively correlated with anxiety in women but inversely correlated with anxiety in men, a finding hypothesized to be due to the modulation of NUCB2 action by sex steroids.[147] As its homolog, NUCB1 is thus a plausible mediator of sex steroid-dependent mood symptoms in PMDD. Furthermore, both NUCB1 and NUCB2 can be quantified in human serum, suggesting its potential as a biomarker for PMDD – a useful application given the difficulty of clinically diagnosing PMDD in the community setting.[3,148,149]

In designing a functional assay to examine phenotypic differences between PMDD and control LCLs, we chose to focus on intracellular calcium homeostasis and, in particular, the ER stress response for several reasons: 1. Of the plausible pathways suggested by our transcriptomic analysis, intracellular calcium handling was the most readily assayable phenotype in LCLs that also had direct implications for neurotransmission and vesicle trafficking. 2. the ER stress response is a robust cellular response to intracellular calcium perturbations, and easily quantified by qPCR measurement of XBP1 splicing.[90,101] 3. NUCB1, a validated E2-DRG, not only regulates intracellular calcium concentrations, but also the ER stress response,[135,143] and 4. differences in intracellular calcium dynamics, including ER stress, in LCL models of psychiatric disease have been previously studied, providing helpful technical precedent.[150–152]

We chose treatment with E2 rather than P4 as the hormone condition used in our Tg challenge experiments based on evidence that response to E2 better stratified LCL transcriptomes by diagnosis (**Figure 1b, Supplemental Figure S1)**. While P4 is an important hormone in the pathophysiology of PMDD, and arguably may have a larger role in precipitating PMDD symptoms,[25,30,38,153] one reason for the primacy of E2 in LCLs is that while LCLs express membrane receptors for progesterone (PGMRC1 and PGMRC2), they do not express PGR, the nuclear progesterone receptor which directly binds DNA to modulate transcription. Expression of nuclear estrogen receptors ESR1 and ESR2, however, is abundant (**Supplemental Figure S2**).

Results of our Tg challenge experiments suggest that, while control LCLs demonstrate an initiation of the ER stress response upon Tg treatment and a positive modulation of this response by E2, both the ER stress response and its modulation by E2 are diminished or absent in PMDD LCLs under the tested conditions. Interestingly, the blunting of the ER stress response seen PMDD LCLs parallels similar results reported in LCLs from people with bipolar disorder (BD). Using a similar experimental design, So et al found attenuated XBP1 induction in BD LCLs compared to control LCLs. Even with a higher dose and longer exposure time (0.3 uM for 6h, verses 0.2 uM for 4h as in our study), XBP1 induction was only modest in BD LCLs (< 2-fold), compared to control LCLs (> 3 fold).[150] Analogous findings of an impaired or absent ER stress response in cultured LCLs from patients with BD were later independently reported by Hayashi et al and Pfaffenseller et al.[151,152]

The ER stress response, also known as the unfolded protein response, is a robust and highly conserved cellular response to the accumulation of misfolded proteins in the endomembrane system, and entails the rapid production of protein folding chaperones, halting

of ribosomal translation, upregulated proteolysis, and increased transport of calcium ions between the cytoplasm and endomembrane organelles such as the ER, Golgi, and mitochondria.[154–157] The ER stress response has many triggers, including inflammation, cellular injury, and stress, with altered intracellular calcium being the most important experimental agent used in the study of the ER stress response.[157,158]

Associations between the ER stress response and other mood and stress-related disorders have been investigated. For example, while the aforementioned studies have reported a decreased ER stress response associated with BD, increased markers of ER stress have been found in the hippocampi of a rat model of learned helplessness,[159] the temporal cortex of people with major depression and completed suicide,[160] and leukocytes of people with major depression in a community setting.[69] Whether the ER stress response is shown to be diminished or augmented in psychiatric disease may depend on the diagnosis, the tissues or cellular systems studied, and the nature and chronicity of stress exposure; failure to mount an adequate homeostatic response to an acute ER stressor such as Tg in an in-vitro system may also be associated with increased ER stress markers in the setting of chronic stress seen in animal and human subjects.

More fundamentally, because of the central role of the ER stress response in intracellular calcium homeostasis, aberrant intracellular calcium handling is one mechanism by which altered ER stress is thought to produce vulnerability to psychiatric disease. Indeed, impaired intracellular calcium homeostasis is the best characterized cellular perturbations in bipolar disorder.[161–164] The ER stress response pathway is also targeted by many mood stabilizing drugs,[165,166] and there exists ample clinical precedent for targeting cellular calcium in the treatment of mood disorders, including the once routine use of calcium channel blockers for treating depression and bipolar disorder.[167,168] L-type calcium channel antagonists have been used in the treatment of bipolar disorder, albeit off-label, since the 1980s, and while their efficacious use has been overshadowed and supplanted by more conventional mood stabilizers, they nonetheless are an evidence-based treatment option for mood disorders.[168] The metabolism of calcium, along with magnesium, have previously been implicated in affective conditions including PMS and PMDD, with some studies documenting differences in serum free ionized calcium and urinary calcium excretion during the luteal phase in women with PMDD, and others suggesting that calcium supplementation may be useful in alleviating symptoms of PMS and PMDD,[169–171] though, the evidence for this is mixed and limited. It is also important to note that the regulation of intracellular calcium is related to, but mechanistically distinct from, the regulation of serum or total body calcium. Nonetheless, the role of divalent cations such as

calcium, magnesium, and lithium in the regulation of mood and behavior has been a topic of longstanding research interest.[172–174] Of note, one mechanism by which lithium, a common and efficacious first-line treatment option for bipolar disorder and add-on augmentation for SSRI-resistant depression, is thought to exert its therapeutic effect is through modulation of the ER stress response.[172,175,176] If confirmed in future studies, hormone-dependent alterations in the ER stress response and calcium homeostasis represent a novel yet conceptually plausible pathway in the pathophysiology of PMDD.

This study has several limitations. Our findings of hormone-dependent differences in calcium homeostasis implicate a relevant and plausible pathway in the pathophysiology of PMDD, but do so in a modest sample size of 13 patient-derived LCLs (6 controls and 7 cases). Cell lines used in the Tg challenge experiments were selected by convenience and were not completely independent from the cell lines used to generate our initial RNAseq data. Generalizability of these results will be supported by validation in larger, independent cohorts.

Our findings of altered calcium homeostasis and ER stress response require mechanistic follow-up. By relying on XBP1 splicing as the sole functional output in our Tg challenge experiments, we were unable to investigate intracellular calcium homeostasis and the ER stress response as separate physiologic processes. Objective measurement of intracellular calcium fluxes through calcium imaging or electrophysiology experiments, and more comprehensive studies of ER stress markers (e.g. GRP94, GRP78, CHOP, c-Fos, etc.) would allow for a better mechanistic understanding of altered calcium dynamics and ER stress in PMDD. Finally, the potential role of NUCB1 – a promising lead given its successful validation as an E2-DRG – in modulating intracellular calcium homeostasis in PMDD is another area for future experimentation.

The interpretation of our module-level analysis of LCL transcriptomes should also be qualified. Functional analysis of differentially regulated modules was performed through gene set enrichment analysis tools, which we primarily employed for data exploration and hypothesis generation. Our decision to select Leading Edge genes for further enrichment analysis, while a reasonable method of isolating ontologically and statistically important genes within a module, also introduces a potential selection bias. Thus, our functional enrichment analyses of WGCNA modules are not in themselves definitive implications of certain cellular or biochemical pathways in PMDD. In particular, while the isolation of the neuronally-relevant magenta module was helpful for informing the design of our Tg challenge assays and has interesting implications for the use of LCLs as a model of neuropsychiatric disease, we cannot conclude that this module is the transcriptional basis of altered calcium homeostasis in PMDD. Indeed, our hypothesis of

altered calcium homeostasis is more strongly justified by our gene-level analysis that identified and validated NUCB1 as an E2-DRG, more so than our module-level analysis identifying enriched calcium-related pathways among core LEA genes of the magenta module.

Nonetheless, our analysis of differentially responsive modules suggests interesting questions for further exploration. For example, future work could investigate the potential coordinated role of the proteasome with epigenetic modifiers such as the ESC/E(Z) complex in modulating the cellular response to ovarian steroids – a hypothesis suggested by our functional analysis of the turquoise module. The potential regulatory relationship between the ESC/E(Z) complex and other genes of the turquoise module and calcium-regulating genes of the magenta module, as suggested by the results of our transcription factor target enrichment analysis, can also be studied to better understand the mechanistic basis of altered calcium homeostasis in PMDD. While WGCNA analysis can suggest the coregulatory architecture of genes modules implicated in PMDD, integration of these results with genetic data may help uncover the genetic basis of altered gene regulation and hormone response in PMDD.

Finally, we do not assume that LCLs are an authentic model of neuronal function, much less mood and behavior.[52–54] While our transcriptomic and functional exploration of LCLs reveals potentially relevant differences in intrinsic cellular traits, a more complete understanding of PMDD will require experiments in more neuronally-relevant samples, such as neuronal cell lines derived from patient-derived induced pluripotent stem cells or postmortem brain tissue.

Summary

This is the first study to report, at the intrinsic cellular level, the molecular and functional correlates of the differential hormone response hypothesized to be central to the pathophysiology of PMDD, and to demonstrate a functional difference between the cells of women with PMDD and asymptomatic controls that appears to be modulated by hormone exposure. Our finding that PMDD LCLs exhibit a blunting of the E2-dependent ER stress response parallels similar reports of ER-stress response impairment in major depression and particularly bipolar disorder—clinical syndromes with which the symptomatic phase of PMDD shares considerable phenomenological overlap. Our transcriptomic analysis also expands on the previously published finding that the ESC/E(Z) complex is differentially expressed between PMDD and control LCLs at baseline. Through the identification of a differentially regulated, neuronally relevant gene module enriched for targets of the same transcriptional modifiers (SUZ12, EZH2) and histone marker (H3K27me3) associated with the ESC/E(Z) complex, we identify a plausible mechanism by which baseline differences in ESC/E(Z) complex expression

leads to a pathologic transcriptomic response upon exposure to hormone. More broadly, through the isolation of a discrete genetic module highly enriched for genes related to neuronal and synaptic functions, we provide evidence for the relevance of LCLs as a model system for the study of neuropsychiatric disease.

Funding Information

This research was supported by the Intramural Research Program of the NIMH, NIH. NIMH Protocols 90-M-0088, 92-M-0174; Project # MH002865. HJL was also supported by the Harvard Medical School Scholars in Medicine Office.

Acknowledgements

We thank Cheryl Marrieta, Longina Akhtar, Maria Mazzu, and Dion Hipolito for technical assistance, and Dr. Sarah Rudzinskas, Dr. Yonwoo Jung, Dr. Qiaoping Yuan, and Allison Goff for helpful discussions. We also thank Karla Thompson and Linda Schenkel for their clinical support and data management, and Catherine Roca who initiated the PMDD genetics project and was responsible for collecting many of the samples employed in the replication sample for this study. This work was written as part of Peter J. Schmidt's official duties as a Government employee. The views expressed in this article do not necessarily represent the views of the NIMH, NIH, HHS, or the United States Government.

Figure Legends

Figure 1. RNAseq analysis workflow.

RNAseq data from patient-derived LCLs under untreated, E2-treated, and P4-treated conditions were analysed using two approaches: (1) In a module-level analysis, Weighted Gene Correlation Network Analysis (WGCNA) was used to identify differentially regulated modules. The functions of these modules were explored for functional enrichment using GSEA. One module of interest (Magenta) was further analyzed using Leading Edge Analysis (LEA) to identify a core set of genes underlying the enrichment signals identified in GSEA. These LEA genes were then analyzed for functional enrichment in Enrichr to discover potential physiologic pathways for downstream experiments. (2) In a gene-level analysis, EdgeR was used to fit a linear model to RNAseq data to identify individual genes that were differentially regulated by E2 (E2-DRGs) or P4 (P4-DRGs). Select DRGs were then explored with network visualization in GeneMANIA and validating using qPCR. Review of validated DRGs and resultant network could then be used to inform the design of a physiologic in-vitro assay.

Figure 2. Functional analysis of WGCNA modules.

a. Cluster dendrogram of genes modules. In WGCNA analysis of 46 input transcriptomes, 21 746 genes were clustered into 65 modules.

b. Module eigengenes showing significant diagnosis x hormone interactions. In ANOVA analysis of module eigengenes, the Brown, Pink, Turquoise, and Magenta module eigengenes showed differential regulation by hormone (Interaction P-value < 0.05). Closed circles denote control samples. Open circles denote PMDD samples. Note: One extreme upper outlier in the E2-treated control group was excluded in the eigengene plot of the Magenta module for scaling purposes. Hormone x diagnosis interaction was significant both before and after exclusion of this data point.

c. Module membership of ESC/E(Z) complex genes. Nearly half of all ESC/E(Z) complex genes (6 of 13) were clustered into the Turquoise module. Other genes were clustered into the Blue, AntiqueWhite4 (aw4), DarkOliveGreen (dog), Cyan (cy), Green (g), and and SkyBlue2 (sb2) modules.

d. ESC/E(Z) complex genes in the Turquoise module. Plot of Turquoise module genes, based on module membership and association with diagnosis (control vs. PMDD). ESC/E(Z) complex genes (SUZ12, EED, AEBP2, HDAC2, MTF2, SIRT2) are more likely to be high connectivity, high significance of the Turquoise module.

e. Word cloud representations of GSEA results. Top 20 GSEA results were used to generate word clouds for each differentially regulated module, which were enriched for terms relating to MAP Kinase and GTPase signaling (Brown, top left), chromatin remodeling and proteasome function (Turquoise, top right), mitochondrial function (Pink, bottom left), and neuronal and synaptic function (Magenta, bottom right). Full GSEA results are tabulated in Supplemental Table S3.

Figure 3. Enrichr analysis of Magenta module LEA genes.

Magenta module genes isolated by Leading Edge Analysis were inputted into Enrichr for functional enrichment analysis against 6 datasets: **a.** ENCODE and ChEA Consensus TFs from ChIP-X, **b.** NIH Roadmap Epigenomics Histone Modification ChIP-seq data set, **c.** KEGG cell signaling pathways (2016), and GO terms for **d.** Biological Processes, **e.** Molecular Function, and **f.** Cellular Component (2018). Bars are proportional to Combined Score Ranking, a composite score proportional to the log P-value of significance using the Fisher Exact Test, and the Z-score of deviation from expected rank. Calcium-relevant pathways are highlighted in blue.

Figure 4. Network analysis and qPCR validation of Top E2-DRGs.

a. GeneMANIA visualization of select E2-DRGs. Key genes relating to ER-Golgi function and intracellular calcium homeostasis (NUCB1, GCC2, GOLGB1) were selected from among the top

10 E2-DRGs and included as inputs for GeneMANIA network visualization, along with DHCR7, a key gene in regulating cholesterol, Vitamin D synthesis, and extracellular calcium balance. TRPM7, another significant E2-DRG ($p = 0.008$) that codes for a cation channel responsible for regulated calcium entry into the cytosol, was also included as an input. The resulting output revealed a structural network of Golgi-ER-associated genes, with physical interactions comprising 67.6% of the weighted network.

b. qPCR validation of select E2-DRGs. NUCB1, DHCR7, PPP2R5D, and GOLGB1 were selected for qPCR validation in an independent replication cohort of 13 cases and 13 controls. NUCB1 qPCR measures a significant interaction of diagnosis and hormone treatment ($F(1, 24) = 7.008$, $p = 0.0141$), and E2-treated PMDD samples had significantly reduced NUCB1 expression compared to control samples ($p = 0.0030$). DHCR7 expression was significantly reduced in E2-treated PMDD samples compared to E2-treated control samples ($p = 0.0395$). No significant results were found in qPCR validation for PPP2R5D or GOLGB1.

Figure 5. Thapsigargin (Tg) challenge assays.

a. Experimental design of Tg challenge assays. PMDD and Control LCLs were each divided into four treatment groups, and cultured in phenol-free RPMI for 5-6 days. One group received no treatment. Another group was exposed to E2 (100 nM) for 24 hours. Another group was exposed to Tg (0.2 uM) for 4 hours. Finally, another group was exposed to E2 (100 nM) for 24 hours, and Tg (0.2 uM) and $CaCl_2$ (0.8 mM) for the last 4 hours. Cells were then harvested and assayed for the spliced-to-unspliced XBP1 by qPCR.

b. XBP1 S/US ratios in Tg challenge assays. While Control LCLs showed an increase in the XBP1 S/US ratio with Tg treatment, and pre-treatment with E2 potentiated this response, both of these effects were blunted or absent in PMDD LCLs. ANOVA-RM analysis of qPCR results showed a significant Diagnosis x Treatment interaction ($F(3,33) = 3.508$, $P = 0.0259$). Post-hoc analysis revealed a significant difference between control and PMDD LCLs only when cells were treated with the combination of E2 + Tg ($p = 0.005$).

Supplemental Figure S1. Response to E2, not P4, underlies the differential hormone response in PMDD.

a. Hierarchical clustering of transcriptomes shows that 1. E2-treated samples cluster more strongly together than P4-treated samples, and 2. Within the E2-treated cluster, there is greater segregation of samples by diagnosis.

b. Plot of modules by ANOVA results, with significance of main effect of diagnosis on the x-axis, and significance of diagnosis x hormone interaction on the y-axis (- log P-value). Size of each point is proportional to the enrichment ratio of E2-DRGs (left) or P4-DRGs (right). The enrichment ratio is calculated by computing the observed / expected proportion of DRGs in each module.

Table Legends

Table 1. Tabulated ANOVA P-values for effects of diagnoses and hormone treatment on module eigengene expression. Eigengene expression values were extracted from all 46 input samples across all 65 modules. Two-way ANOVA analysis was performed to quantify the effects of Diagnosis, Hormone Treatment, and their interaction. Four modules (Brown, Pink, Turquoise, and Magenta) showed significant effects of Diagnosis x Hormone interactions.

Table 2. Top 10 genes differentially regulated by E2 in PMDD.

Top 10 most significant genes in EdgeR analysis of genes differentially regulated by E2 in PMDD (E2-DRGs). Genes related to intracellular calcium homeostasis, the Golgi-ER compartment, and the ER stress response are bolded (NUCB1, GCC2, GOLGB1). Genes of potential neurological significance are italicized (DST, PPP2R5D).

Supplemental Table S1. Demographics of women contributing LCL cell lines for each study component. Demographic variables of women with PMDD and healthy controls contributing cell lines are reported for each study component: RNAseq analysis, qPCR validation, and Tg challenge assays. For all study components, no significant differences were found in race/ethnicity, age, BMI, obstetrical history (parity), past psychiatric history (history of major depressive episodes, and history of psychotropic medication use), with the exception of age in the qPCR validation cohort; women in the PMDD group were significantly older than women in the control group ($p = 0.0003$). For each study component, women in the PMDD group more frequently had a history of prior major depressive episodes, but this difference was not statistically significant.

Supplemental Table S2. Input RNAseq samples for WGCNA analysis. A total for 46 replicates, representing 9 control LCLs and 10 PMDD LCLs across untreated, E2-treated, and P4-treated conditions were used for WGCNA analysis. This is in excess of the recommended minimum number of 15 replicates for reliable module detection in WGCNA analysis.

Supplemental Table S3. Top 20 GSEA results for Turquoise, Brown, Pink, and Magenta modules. Modules with eigengenes showing a significant diagnosis x hormone interaction were selected for subsequent analysis in GSEA. Module genes were pre-ranked by the WGCNA intramodular connectivity metric to prioritize high-connectivity hub genes, and pre-ranked lists were analyzed against the C5 Gene Ontology gene sets with 1000 permutations. Gene sets enriched at an FDR-corrected q-values < 0.25 were considered significant. Word frequencies from names of enriched gene sets were used to generate word clouds shown in Figure 2e.

Supplemental Table S4. Leading edge analysis of top 20 Magenta module GSEA GO terms. Top 20 GO terms from GSEA analysis of the magenta module were selected for leading edge analysis (LEA). Leading edge analysis of each enriched gene set yielded a core set of high-ranked (high-connectivity) genes that contributed most to the enrichment signal. The union of these 20 core sets (one for each enriched GO term) comprised 88 LEA genes.

Supplemental Table S5. Enrichr analysis of Magenta LEA genes. Magenta LEA genes were inputted into Enrichr for overlap analysis against four databases: 1. ENCODE and ChEA Consensus TFs from ChIP-X, 2. NIH Roadmap Epigenomics Histone Modification ChIP-seq data set, 3. KEGG's cell signaling pathways (2016), and GO terms for Biological Processes, Molecular Function, and Cellular Component (2018). Magenta LEA genes were enriched for targets of EZH2, SUZ12, and ESR1, as well several pathways related to calcium transport, signaling, and homeostasis. Analysis was performed in December 2018.

Supplemental Table S6-S7. EdgeR output for significant DRGs. In EdgeR, paired RNAseq samples were fitted to a quasi-likelihood negative binomial generalized log-linear model in which the factors of subject (cell line) and treatment (untreated vs. hormone-treated) were both nested under diagnosis (control vs. PMDD). Genewise F-tests were conducted to identify genes showing significant diagnosis x hormone interactions (nominal $P < 0.05$). This analysis was performed for both E2-treated and P4-treated samples, yielding a list of genes differentially responsive to E2 (E2-DRGs) and to P4 (P4-DRGs).

Supplemental Table S8. Repeated measures ANOVA analysis of Tg challenge experiments. PMDD LCLs exhibit a blunted XBP1 splicing response to Tg compared to control LCLs, and this effect is accentuated when LCLs were pre-treated with estradiol prior to Tg

exposure. Analysis of XBP1 splice-to-unspliced ratios show a significant main effect of treatment ($F(3,33) = 11.22$, $P < 0.001$), and a significant diagnosis x treatment interaction ($F(3,33) = 3.508$, $P = 0.0259$). The effect of diagnosis was nearly significant ($F(1,11) = 4.25$, $P = 0.0637$). In post-hoc analysis, control LCLs had a 1.7-fold increase in XBP1 splicing from baseline with Tg alone ($p = 0.0085$), and a 2.2-fold increase with Tg preceded by E2 ($p < 0.0001$). In contrast, PMDD LCLs showed a blunted, non-significant increase in XBP1 splicing in both conditions. Comparing PMDD and control LCLs within treatment conditions, the splicing response of PMDD LCLs was 1.36-fold decreased compared to control LCLs in the Tg-only condition ($p = 0.25$), and this difference was accentuated and significant when Tg was preceded by E2, with a 1.62-fold decreased splicing response ($p = 0.005$).

References

1. Hofmeister, S. & Bodden, S. Premenstrual Syndrome and Premenstrual Dysphoric Disorder. *Am. Fam. Physician* **94**, 236–240 (2016).
2. O'Brien, P. M. S. *et al.* Towards a consensus on diagnostic criteria, measurement and trial design of the premenstrual disorders: the ISPMD Montreal consensus. *Arch. Womens Ment. Health* **14**, 13–21 (2011).
3. Eisenlohr-Moul, T. A. *et al.* Toward the Reliable Diagnosis of DSM-5 Premenstrual Dysphoric Disorder: The Carolina Premenstrual Assessment Scoring System (C-PASS). *Am. J. Psychiatry* **174**, 51–59 (2017).
4. Halbreich, U., Borenstein, J., Pearlstein, T. & Kahn, L. S. The prevalence, impairment, impact, and burden of premenstrual dysphoric disorder (PMS/PMDD). *Psychoneuroendocrinology* **28**, 1–23 (2003).
5. Daw, J. Is PMDD real? *Monit. Psychol. - Am. Psychol. Assoc.* **33**, 58 (2002).
6. Hartlage, S. A., Breaux, C. A. & Yonkers, K. A. Addressing concerns about the inclusion of premenstrual dysphoric disorder in DSM-5. *J. Clin. Psychiatry* **75**, 70–76 (2014).
7. Rapkin, A. J. & Winer, S. A. Premenstrual syndrome and premenstrual dysphoric disorder: quality of life and burden of illness. *Expert Rev. Pharmacoecon. Outcomes Res.* **9**, 157–170 (2009).
8. Yang, M. *et al.* Burden of premenstrual dysphoric disorder on health-related quality of life. *J. Womens Health 2002* **17**, 113–121 (2008).
9. Dean, B. B. & Borenstein, J. E. A prospective assessment investigating the relationship between work productivity and impairment with premenstrual syndrome. *J. Occup. Environ. Med.* **46**, 649–656 (2004).

10. Borenstein, J., Chiou, C.-F., Dean, B., Wong, J. & Wade, S. Estimating direct and indirect costs of premenstrual syndrome. *J. Occup. Environ. Med.* **47**, 26–33 (2005).
11. Pilver, C. E., Libby, D. J. & Hoff, R. A. Premenstrual dysphoric disorder as a correlate of suicidal ideation, plans, and attempts among a nationally representative sample. *Soc. Psychiatry Psychiatr. Epidemiol.* **48**, 437–446 (2013).
12. Kessler, R. C., Borges, G. & Walters, E. E. Prevalence of and risk factors for lifetime suicide attempts in the National Comorbidity Survey. *Arch. Gen. Psychiatry* **56**, 617–626 (1999).
13. Epperson, C. N. *et al.* Premenstrual dysphoric disorder: evidence for a new category for DSM-5. *Am. J. Psychiatry* **169**, 465–475 (2012).
14. Yen, J.-Y. *et al.* Estrogen levels, emotion regulation, and emotional symptoms of women with premenstrual dysphoric disorder: The moderating effect of estrogen receptor 1α polymorphism. *Prog. Neuropsychopharmacol. Biol. Psychiatry* **82**, 216–223 (2018).
15. Akturk, M. *et al.* Circulating insulin and leptin in women with and without premenstrual disphoric disorder in the menstrual cycle. *Gynecol. Endocrinol. Off. J. Int. Soc. Gynecol. Endocrinol.* **29**, 465–469 (2013).
16. Hsiao, C.-C., Liu, C.-Y. & Hsiao, M.-C. No correlation of depression and anxiety to plasma estrogen and progesterone levels in patients with premenstrual dysphoric disorder. *Psychiatry Clin. Neurosci.* **58**, 593–599 (2004).
17. Giannini, A. J., Martin, D. M. & Turner, C. E. Beta-endorphin decline in late luteal phase dysphoric disorder. *Int. J. Psychiatry Med.* **20**, 279–284 (1990).
18. Schiller, C. E., Johnson, S. L., Abate, A. C., Schmidt, P. J. & Rubinow, D. R. Reproductive Steroid Regulation of Mood and Behavior. *Compr. Physiol.* **6**, 1135–1160 (2016).
19. Rubinow, D. R., Schmidt, P. J. & Roca, C. A. Hormone measures in reproductive endocrine-related mood disorders: diagnostic issues. *Psychopharmacol. Bull.* **34**, 289–290 (1998).
20. Hantsoo, L. & Epperson, C. N. Premenstrual Dysphoric Disorder: Epidemiology and Treatment. *Curr. Psychiatry Rep.* **17**, 87 (2015).
21. Schmidt, P. J., Nieman, L. K., Danaceau, M. A., Adams, L. F. & Rubinow, D. R. Differential behavioral effects of gonadal steroids in women with and in those without premenstrual syndrome. *N. Engl. J. Med.* **338**, 209–216 (1998).
22. Schmidt, P. J. *et al.* Premenstrual Dysphoric Disorder Symptoms Following Ovarian Suppression: Triggered by Change in Ovarian Steroid Levels But Not Continuous Stable Levels. *Am. J. Psychiatry* **174**, 980–989 (2017).

23. Baller, E. B. *et al.* Abnormalities of dorsolateral prefrontal function in women with premenstrual dysphoric disorder: a multimodal neuroimaging study. *Am. J. Psychiatry* **170**, 305–314 (2013).
24. Protopopescu, X. *et al.* Toward a functional neuroanatomy of premenstrual dysphoric disorder. *J. Affect. Disord.* **108**, 87–94 (2008).
25. Gingnell, M., Morell, A., Bannbers, E., Wikström, J. & Sundström Poromaa, I. Menstrual cycle effects on amygdala reactivity to emotional stimulation in premenstrual dysphoric disorder. *Horm. Behav.* **62**, 400–406 (2012).
26. Toffoletto, S., Lanzenberger, R., Gingnell, M., Sundström-Poromaa, I. & Comasco, E. Emotional and cognitive functional imaging of estrogen and progesterone effects in the female human brain: a systematic review. *Psychoneuroendocrinology* **50**, 28–52 (2014).
27. Gingnell, M. *et al.* Social stimulation and corticolimbic reactivity in premenstrual dysphoric disorder: a preliminary study. *Biol. Mood Anxiety Disord.* **4**, 3 (2014).
28. Petersen, N. *et al.* Brain activation during emotion regulation in women with premenstrual dysphoric disorder. *Psychol. Med.* **48**, 1795–1802 (2018).
29. Stickel, S. *et al.* Neural correlates of depression in women across the reproductive lifespan - An fMRI review. *J. Affect. Disord.* **246**, 556–570 (2018).
30. Bixo, M., Johansson, M., Timby, E., Michalski, L. & Bäckström, T. Effects of GABA active steroids in the female brain with a focus on the premenstrual dysphoric disorder. *J. Neuroendocrinol.* **30**, (2018).
31. Wilson, C. A., Turner, C. W. & Keye, W. R. Firstborn adolescent daughters and mothers with and without premenstrual syndrome: a comparison. *J. Adolesc. Health Off. Publ. Soc. Adolesc. Med.* **12**, 130–137 (1991).
32. Kendler, K. S. *et al.* Genetic and environmental factors in the aetiology of menstrual, premenstrual and neurotic symptoms: a population-based twin study. *Psychol. Med.* **22**, 85–100 (1992).
33. Kendler, K. S., Karkowski, L. M., Corey, L. A. & Neale, M. C. Longitudinal population-based twin study of retrospectively reported premenstrual symptoms and lifetime major depression. *Am. J. Psychiatry* **155**, 1234–1240 (1998).
34. Huo, L. *et al.* Risk for premenstrual dysphoric disorder is associated with genetic variation in ESR1, the estrogen receptor alpha gene. *Biol. Psychiatry* **62**, 925–933 (2007).
35. Schüle, C., Nothdurfter, C. & Rupprecht, R. The role of allopregnanolone in depression and anxiety. *Prog. Neurobiol.* **113**, 79–87 (2014).

36. Bali, A. & Jaggi, A. S. Multifunctional aspects of allopregnanolone in stress and related disorders. *Prog. Neuropsychopharmacol. Biol. Psychiatry* **48**, 64–78 (2014).
37. Bäckström, T. *et al.* Paradoxical effects of GABA-A modulators may explain sex steroid induced negative mood symptoms in some persons. *Neuroscience* **191**, 46–54 (2011).
38. Andréen, L. *et al.* Sex steroid induced negative mood may be explained by the paradoxical effect mediated by GABAA modulators. *Psychoneuroendocrinology* **34**, 1121–1132 (2009).
39. Harrisberger, F. *et al.* BDNF Val66Met polymorphism and hippocampal volume in neuropsychiatric disorders: A systematic review and meta-analysis. *Neurosci. Biobehav. Rev.* **55**, 107–118 (2015).
40. Wei, S.-M. *et al.* Brain-derived neurotrophic factor Val66Met genotype and ovarian steroids interactively modulate working memory-related hippocampal function in women: a multimodal neuroimaging study. *Mol. Psychiatry* **23**, 1066–1075 (2018).
41. Wei, S.-M. & Berman, K. F. Ovarian hormones, genes, and the brain: the case of estradiol and the brain-derived neurotrophic factor (BDNF) gene. *Neuropsychopharmacol. Off. Publ. Am. Coll. Neuropsychopharmacol.* **44**, 223–224 (2019).
42. Marrocco, J. *et al.* Epigenetic intersection of BDNF Val66Met genotype with premenstrual dysphoric disorder transcriptome in a cross-species model of estradiol add-back. *Mol. Psychiatry* (2018). doi:10.1038/s41380-018-0274-3
43. Cubeddu, A. *et al.* Brain-derived neurotrophic factor plasma variation during the different phases of the menstrual cycle in women with premenstrual syndrome. *Psychoneuroendocrinology* **36**, 523–530 (2011).
44. Oral, E. *et al.* Serum brain-derived neurotrophic factor differences between the luteal and follicular phases in premenstrual dysphoric disorder. *Gen. Hosp. Psychiatry* **37**, 266–272 (2015).
45. O'Brien, S. M. *et al.* Impact of gender and menstrual cycle phase on plasma cytokine concentrations. *Neuroimmunomodulation* **14**, 84–90 (2007).
46. Gaskins, A. J. *et al.* Endogenous reproductive hormones and C-reactive protein across the menstrual cycle: the BioCycle Study. *Am. J. Epidemiol.* **175**, 423–431 (2012).
47. Bertone-Johnson, E. R. *et al.* Association of inflammation markers with menstrual symptom severity and premenstrual syndrome in young women. *Hum. Reprod. Oxf. Engl.* **29**, 1987–1994 (2014).
48. Jaremka, L. M., Lindgren, M. E. & Kiecolt-Glaser, J. K. Synergistic relationships among stress, depression, and troubled relationships: insights from psychoneuroimmunology. *Depress. Anxiety* **30**, 288–296 (2013).

49. Kiecolt-Glaser, J. K., Derry, H. M. & Fagundes, C. P. Inflammation: depression fans the flames and feasts on the heat. *Am. J. Psychiatry* **172**, 1075–1091 (2015).
50. Oh, H.-M. *et al.* An efficient method for the rapid establishment of Epstein-Barr virus immortalization of human B lymphocytes. *Cell Prolif.* **36**, 191–197 (2003).
51. Wheeler, H. E. & Dolan, M. E. Lymphoblastoid cell lines in pharmacogenomic discovery and clinical translation. *Pharmacogenomics* **13**, 55–70 (2012).
52. Sie, L., Loong, S. & Tan, E. K. Utility of lymphoblastoid cell lines. *J. Neurosci. Res.* **87**, 1953–1959 (2009).
53. Cai, C. *et al.* Is human blood a good surrogate for brain tissue in transcriptional studies? *BMC Genomics* **11**, 589 (2010).
54. Gladkevich, A., Kauffman, H. F. & Korf, J. Lymphocytes as a neural probe: potential for studying psychiatric disorders. *Prog. Neuropsychopharmacol. Biol. Psychiatry* **28**, 559–576 (2004).
55. Holcombe, R. F., Jones, K. L. & Stewart, R. M. Lysosomal enzyme activities in Chediak-Higashi syndrome: evaluation of lymphoblastoid cell lines and review of the literature. *Immunodeficiency* **5**, 131–140 (1994).
56. Battisti, C. *et al.* Lymphoblastoid cell lines of Rett syndrome patients exposed to oxidative-stress-induced apoptosis. *Brain Dev.* **26**, 384–388 (2004).
57. Lopez-Atalaya, J. P. *et al.* Histone acetylation deficits in lymphoblastoid cell lines from patients with Rubinstein-Taybi syndrome. *J. Med. Genet.* **49**, 66–74 (2012).
58. Liao, D.-L., Cheng, M.-C., Lai, C.-H., Tsai, H.-J. & Chen, C.-H. Comparative gene expression profiling analysis of lymphoblastoid cells reveals neuron-specific enolase gene (ENO2) as a susceptibility gene of heroin dependence. *Addict. Biol.* **19**, 102–110 (2014).
59. Sanders, A. R. *et al.* Transcriptome study of differential expression in schizophrenia. *Hum. Mol. Genet.* **22**, 5001–5014 (2013).
60. Duan, J. *et al.* Transcriptomic signatures of schizophrenia revealed by dopamine perturbation in an ex vivo model. *Transl. Psychiatry* **8**, (2018).
61. Rose, S. *et al.* Oxidative stress induces mitochondrial dysfunction in a subset of autistic lymphoblastoid cell lines. *Transl. Psychiatry* **4**, e377 (2014).
62. Breen, M. S. *et al.* Lithium-responsive genes and gene networks in bipolar disorder patient-derived lymphoblastoid cell lines. *Pharmacogenomics J.* **16**, 446–453 (2016).
63. Kittel-Schneider, S. *et al.* Lithium-induced Clock Gene Expression in Lymphoblastoid Cells of Bipolar Affective Patients. *Pharmacopsychiatry* **48**, 145–149 (2015).

64. Morrison, G. *et al.* Utility of patient-derived lymphoblastoid cell lines as an ex vivo capecitabine sensitivity prediction model for breast cancer patients. *Oncotarget* **7**, 38359–38366 (2016).
65. Niu, N. & Wang, L. In vitro human cell line models to predict clinical response to anticancer drugs. *Pharmacogenomics* **16**, 273–285 (2015).
66. Dubey, N. *et al.* The ESC/E(Z) complex, an effector of response to ovarian steroids, manifests an intrinsic difference in cells from women with premenstrual dysphoric disorder. *Mol. Psychiatry* **22**, 1172–1184 (2017).
67. Bhan, A. *et al.* Histone methyltransferase EZH2 is transcriptionally induced by estradiol as well as estrogenic endocrine disruptors bisphenol-A and diethylstilbestrol. *J. Mol. Biol.* **426**, 3426–3441 (2014).
68. Hwang, C. *et al.* EZH2 regulates the transcription of estrogen-responsive genes through association with REA, an estrogen receptor corepressor. *Breast Cancer Res. Treat.* **107**, 235–242 (2008).
69. Nevell, L. *et al.* Elevated systemic expression of ER stress related genes is associated with stress-related mental disorders in the Detroit Neighborhood Health Study. *Psychoneuroendocrinology* **43**, 62–70 (2014).
70. Gonzalez, M. E. *et al.* Downregulation of EZH2 decreases growth of estrogen receptor-negative invasive breast carcinoma and requires BRCA1. *Oncogene* **28**, 843–853 (2009).
71. American Psychiatric Association. *Diagnostic and Statistical Manual of Mental Disorders*. (American Psychiatric Association, 1994).
72. Kim, D. *et al.* TopHat2: accurate alignment of transcriptomes in the presence of insertions, deletions and gene fusions. *Genome Biol.* **14**, R36 (2013).
73. Liao, Y., Smyth, G. K. & Shi, W. The Subread aligner: fast, accurate and scalable read mapping by seed-and-vote. *Nucleic Acids Res.* **41**, e108 (2013).
74. Langfelder, P. & Horvath, S. WGCNA: an R package for weighted correlation network analysis. *BMC Bioinformatics* **9**, 559 (2008).
75. Subramanian, A. *et al.* Gene set enrichment analysis: a knowledge-based approach for interpreting genome-wide expression profiles. *Proc. Natl. Acad. Sci. U. S. A.* **102**, 15545–15550 (2005).
76. Chen, E. Y. *et al.* Enrichr: interactive and collaborative HTML5 gene list enrichment analysis tool. *BMC Bioinformatics* **14**, 128 (2013).
77. Kuleshov, M. V. *et al.* Enrichr: a comprehensive gene set enrichment analysis web server 2016 update. *Nucleic Acids Res.* **44**, W90-97 (2016).

78. Gene Ontology Consortium. Creating the gene ontology resource: design and implementation. *Genome Res.* **11**, 1425–1433 (2001).
79. Gene Ontology Consortium. Gene Ontology Consortium: going forward. *Nucleic Acids Res.* **43**, D1049-1056 (2015).
80. Liberzon, A. *et al.* Molecular signatures database (MSigDB) 3.0. *Bioinforma. Oxf. Engl.* **27**, 1739–1740 (2011).
81. ENCODE Project Consortium. The ENCODE (ENCyclopedia Of DNA Elements) Project. *Science* **306**, 636–640 (2004).
82. Lachmann, A. *et al.* ChEA: transcription factor regulation inferred from integrating genome-wide ChIP-X experiments. *Bioinforma. Oxf. Engl.* **26**, 2438–2444 (2010).
83. Rouillard, A. D. *et al.* The harmonizome: a collection of processed datasets gathered to serve and mine knowledge about genes and proteins. *Database J. Biol. Databases Curation* **2016**, (2016).
84. Bernstein, B. E. *et al.* The NIH Roadmap Epigenomics Mapping Consortium. *Nat. Biotechnol.* **28**, 1045–1048 (2010).
85. Roadmap Epigenomics Consortium *et al.* Integrative analysis of 111 reference human epigenomes. *Nature* **518**, 317–330 (2015).
86. Ogata, H. *et al.* KEGG: Kyoto Encyclopedia of Genes and Genomes. *Nucleic Acids Res.* **27**, 29–34 (1999).
87. Robinson, M. D., McCarthy, D. J. & Smyth, G. K. edgeR: a Bioconductor package for differential expression analysis of digital gene expression data. *Bioinforma. Oxf. Engl.* **26**, 139–140 (2010).
88. McCarthy, D. J., Chen, Y. & Smyth, G. K. Differential expression analysis of multifactor RNA-Seq experiments with respect to biological variation. *Nucleic Acids Res.* **40**, 4288–4297 (2012).
89. Livak, K. J. & Schmittgen, T. D. Analysis of Relative Gene Expression Data Using Real-Time Quantitative PCR and the 2−ΔΔCT Method. *Methods* **25**, 402–408 (2001).
90. Oslowski, C. M. & Urano, F. Measuring ER stress and the unfolded protein response using mammalian tissue culture system. *Methods Enzymol.* **490**, 71–92 (2011).
91. R Core Team. *R: A Language and Environment for Statistical Computing*. (R Foundation for Statistical Computing, 2017).
92. Faouzi, M., Kilch, T., Horgen, F. D., Fleig, A. & Penner, R. The TRPM7 channel kinase regulates store-operated calcium entry. *J. Physiol.* **595**, 3165–3180 (2017).

93. Suzuki, S., Lis, A., Schmitz, C., Penner, R. & Fleig, A. The TRPM7 kinase limits receptor-induced calcium release by regulating heterotrimeric G-proteins. *Cell. Mol. Life Sci. CMLS* **75**, 3069–3078 (2018).
94. Sagara, Y., Wade, J. B. & Inesi, G. A conformational mechanism for formation of a dead-end complex by the sarcoplasmic reticulum ATPase with thapsigargin. *J. Biol. Chem.* **267**, 1286–1292 (1992).
95. Sehgal, P. *et al.* Inhibition of the sarco/endoplasmic reticulum (ER) Ca2+-ATPase by thapsigargin analogs induces cell death via ER Ca2+ depletion and the unfolded protein response. *J. Biol. Chem.* **292**, 19656–19673 (2017).
96. Pozzan, T., Rizzuto, R., Volpe, P. & Meldolesi, J. Molecular and cellular physiology of intracellular calcium stores. *Physiol. Rev.* **74**, 595–636 (1994).
97. Cahalan, M. D. STIMulating store-operated Ca2+ entry. *Nat. Cell Biol.* **11**, 669–677 (2009).
98. Hogan, P. G. & Rao, A. Store-operated calcium entry: mechanisms and modulation. *Biochem. Biophys. Res. Commun.* **460**, 40–49 (2015).
99. Krebs, J., Agellon, L. B. & Michalak, M. Ca2+ homeostasis and endoplasmic reticulum (ER) stress: An integrated view of calcium signaling. *Biochem. Biophys. Res. Commun.* **460**, 114–121 (2015).
100. Kaufman, R. J. Stress signaling from the lumen of the endoplasmic reticulum: coordination of gene transcriptional and translational controls. *Genes Dev.* **13**, 1211–1233 (1999).
101. Yoshida, H., Matsui, T., Yamamoto, A., Okada, T. & Mori, K. XBP1 mRNA is induced by ATF6 and spliced by IRE1 in response to ER stress to produce a highly active transcription factor. *Cell* **107**, 881–891 (2001).
102. Du, J. *et al.* Stuxnet Facilitates the Degradation of Polycomb Protein during Development. *Dev. Cell* **37**, 507–519 (2016).
103. Dantuma, N. P., Groothuis, T. A. M., Salomons, F. A. & Neefjes, J. A dynamic ubiquitin equilibrium couples proteasomal activity to chromatin remodeling. *J. Cell Biol.* **173**, 19–26 (2006).
104. Pinto, M. J. *et al.* The proteasome controls presynaptic differentiation through modulation of an on-site pool of polyubiquitinated conjugates. *J. Cell Biol.* **212**, 789–801 (2016).
105. Wentzel, C., Delvendahl, I., Sydlik, S., Georgiev, O. & Müller, M. Dysbindin links presynaptic proteasome function to homeostatic recruitment of low release probability vesicles. *Nat. Commun.* **9**, 267 (2018).

106. Bach, S. V., Tacon, P. R., Morgan, J. W. & Hegde, A. N. Proteasome regulates transcription-favoring histone methylation, acetylation and ubiquitination in long-term synaptic plasticity. *Neurosci. Lett.* **591**, 59–64 (2015).

107. Ma, Q. *et al.* Proteasome-independent polyubiquitin linkage regulates synapse scaffolding, efficacy, and plasticity. *Proc. Natl. Acad. Sci. U. S. A.* **114**, E8760–E8769 (2017).

108. Ferreira, J. S. *et al.* GluN2B-Containing NMDA Receptors Regulate AMPA Receptor Traffic through Anchoring of the Synaptic Proteasome. *J. Neurosci. Off. J. Soc. Neurosci.* **35**, 8462–8479 (2015).

109. Cheon, S., Dean, M. & Chahrour, M. The ubiquitin proteasome pathway in neuropsychiatric disorders. *Neurobiol. Learn. Mem.* (2018). doi:10.1016/j.nlm.2018.01.012

110. Minelli, A. *et al.* Proteasome system dysregulation and treatment resistance mechanisms in major depressive disorder. *Transl. Psychiatry* **5**, e687 (2015).

111. Scott, M. R., Rubio, M. D., Haroutunian, V. & Meador-Woodruff, J. H. Protein Expression of Proteasome Subunits in Elderly Patients with Schizophrenia. *Neuropsychopharmacol. Off. Publ. Am. Coll. Neuropsychopharmacol.* **41**, 896–905 (2016).

112. Bousman, C. A. *et al.* Positive symptoms of psychosis correlate with expression of ubiquitin proteasome genes in peripheral blood. *Am. J. Med. Genet. Part B Neuropsychiatr. Genet. Off. Publ. Int. Soc. Psychiatr. Genet.* **153B**, 1336–1341 (2010).

113. Altar, C. A. *et al.* Deficient hippocampal neuron expression of proteasome, ubiquitin, and mitochondrial genes in multiple schizophrenia cohorts. *Biol. Psychiatry* **58**, 85–96 (2005).

114. Ross, C. A. & Pickart, C. M. The ubiquitin-proteasome pathway in Parkinson's disease and other neurodegenerative diseases. *Trends Cell Biol.* **14**, 703–711 (2004).

115. Dennis, A. P. & O'Malley, B. W. Rush hour at the promoter: how the ubiquitin-proteasome pathway polices the traffic flow of nuclear receptor-dependent transcription. *J. Steroid Biochem. Mol. Biol.* **93**, 139–151 (2005).

116. Dennis, A. P., Lonard, D. M., Nawaz, Z. & O'Malley, B. W. Inhibition of the 26S proteasome blocks progesterone receptor-dependent transcription through failed recruitment of RNA polymerase II. *J. Steroid Biochem. Mol. Biol.* **94**, 337–346 (2005).

117. Li, X. *et al.* The SRC-3/AIB1 coactivator is degraded in a ubiquitin- and ATP-independent manner by the REGgamma proteasome. *Cell* **124**, 381–392 (2006).

118. Lonard, D. M., Nawaz, Z., Smith, C. L. & O'Malley, B. W. The 26S proteasome is required for estrogen receptor-alpha and coactivator turnover and for efficient estrogen receptor-alpha transactivation. *Mol. Cell* **5**, 939–948 (2000).

119. Einat, H. *et al.* The role of the extracellular signal-regulated kinase signaling pathway in mood modulation. *J. Neurosci. Off. J. Soc. Neurosci.* **23**, 7311–7316 (2003).
120. Quiroz, J. A. *et al.* Emerging experimental therapeutics for bipolar disorder: clues from the molecular pathophysiology. *Mol. Psychiatry* **9**, 756–776 (2004).
121. Duric, V. *et al.* A negative regulator of MAP kinase causes depressive behavior. *Nat. Med.* **16**, 1328–1332 (2010).
122. Watters, J. J., Campbell, J. S., Cunningham, M. J., Krebs, E. G. & Dorsa, D. M. Rapid membrane effects of steroids in neuroblastoma cells: effects of estrogen on mitogen activated protein kinase signalling cascade and c-fos immediate early gene transcription. *Endocrinology* **138**, 4030–4033 (1997).
123. Zhang, L. *et al.* Sex-related differences in MAPKs activation in rat astrocytes: effects of estrogen on cell death. *Brain Res. Mol. Brain Res.* **103**, 1–11 (2002).
124. Shimamoto, A. & Rappeneau, V. Sex-dependent mental illnesses and mitochondria. *Schizophr. Res.* **187**, 38–46 (2017).
125. Allen, J., Romay-Tallon, R., Brymer, K. J., Caruncho, H. J. & Kalynchuk, L. E. Mitochondria and Mood: Mitochondrial Dysfunction as a Key Player in the Manifestation of Depression. *Front. Neurosci.* **12**, 386 (2018).
126. Milanesi, E. *et al.* RNA sequencing of bipolar disorder lymphoblastoid cell lines implicates the neurotrophic factor HRP-3 in lithium's clinical efficacy. *World J. Biol. Psychiatry Off. J. World Fed. Soc. Biol. Psychiatry* 1–13 (2017). doi:10.1080/15622975.2017.1372629
127. Kittel-Schneider, S. *et al.* Lithium-induced gene expression alterations in two peripheral cell models of bipolar disorder. *World J. Biol. Psychiatry Off. J. World Fed. Soc. Biol. Psychiatry* 1–14 (2017). doi:10.1080/15622975.2017.1396357
128. Tylee, D. S. *et al.* RNA sequencing of transformed lymphoblastoid cells from siblings discordant for autism spectrum disorders reveals transcriptomic and functional alterations: Evidence for sex-specific effects. *Autism Res. Off. J. Int. Soc. Autism Res.* **10**, 439–455 (2017).
129. Jong, S. de *et al.* A Gene Co-Expression Network in Whole Blood of Schizophrenia Patients Is Independent of Antipsychotic-Use and Enriched for Brain-Expressed Genes. *PLOS ONE* **7**, e39498 (2012).
130. Scheller, U. *et al.* Integrative bioinformatics analysis characterizing the role of EDC3 in mRNA decay and its association to intellectual disability. *BMC Med. Genomics* **11**, 41 (2018).

131. Kos, M. Z. *et al.* Dopamine perturbation of gene co-expression networks reveals differential response in schizophrenia for translational machinery. *Transl. Psychiatry* **8**, 278 (2018).

132. Margueron, R. & Reinberg, D. The Polycomb complex PRC2 and its mark in life. *Nature* **469**, 343–349 (2011).

133. Di Croce, L. & Helin, K. Transcriptional regulation by Polycomb group proteins. *Nat. Struct. Mol. Biol.* **20**, 1147–1155 (2013).

134. Viré, E. *et al.* The Polycomb group protein EZH2 directly controls DNA methylation. *Nature* **439**, 871 (2006).

135. Lin, P., Yao, Y., Hofmeister, R., Tsien, R. Y. & Farquhar, M. G. Overexpression of CALNUC (Nucleobindin) Increases Agonist and Thapsigargin Releasable Ca2+ Storage in the Golgi. *J. Cell Biol.* **145**, 279–289 (1999).

136. Lin, P. *et al.* The Mammalian Calcium-binding Protein, Nucleobindin (CALNUC), Is a Golgi Resident Protein. *J. Cell Biol.* **141**, 1515–1527 (1998).

137. de Alba, E. & Tjandra, N. Structural Studies on the Ca2+-binding Domain of Human Nucleobindin (Calnuc). *Biochemistry* **43**, 10039–10049 (2004).

138. Gonzalez, R. *et al.* Nesfatin-1 exerts a direct, glucose-dependent insulinotropic action on mouse islet β- and MIN6 cells. *J. Endocrinol.* **208**, R9–R16 (2011).

139. Nakata, M., Manaka, K., Yamamoto, S., Mori, M. & Yada, T. Nesfatin-1 enhances glucose-induced insulin secretion by promoting Ca(2+) influx through L-type channels in mouse islet β-cells. *Endocr. J.* **58**, 305–313 (2011).

140. Ramesh, N., Mohan, H. & Unniappan, S. Nucleobindin-1 encodes a nesfatin-1-like peptide that stimulates insulin secretion. *Gen. Comp. Endocrinol.* **216**, 182–189 (2015).

141. Williams, P., Tulke, S., Ilegems, E., Berggren, P.-O. & Broberger, C. Expression of nucleobindin 1 (NUCB1) in pancreatic islets and other endocrine tissues. *Cell Tissue Res.* **358**, 331–342 (2014).

142. Tulke, S. *et al.* Nucleobindin 1 (NUCB1) is a Golgi-resident marker of neurons. *Neuroscience* **314**, 179–188 (2016).

143. Tsukumo, Y. *et al.* Nucleobindin 1 controls the unfolded protein response by inhibiting ATF6 activation. *J. Biol. Chem.* **282**, 29264–29272 (2007).

144. Sundarrajan, L. *et al.* Nesfatin-1-Like Peptide Encoded in Nucleobindin-1 in Goldfish is a Novel Anorexigen Modulated by Sex Steroids, Macronutrients and Daily Rhythm. *Sci. Rep.* **6**, 28377 (2016).

145. Oh-I, S. *et al.* Identification of nesfatin-1 as a satiety molecule in the hypothalamus. *Nature* **443**, 709–712 (2006).
146. Schalla, M. A. & Stengel, A. Current Understanding of the Role of Nesfatin-1. *J. Endocr. Soc.* **2**, 1188–1206 (2018).
147. Hofmann, T. *et al.* Sex-specific regulation of NUCB2/nesfatin-1: Differential implication in anxiety in obese men and women. *Psychoneuroendocrinology* **60**, 130–137 (2015).
148. Bosman, R. C., Jung, S. E., Miloserdov, K., Schoevers, R. A. & aan het Rot, M. Daily symptom ratings for studying premenstrual dysphoric disorder: A review. *J. Affect. Disord.* **189**, 43–53 (2016).
149. Epperson, C. N. & Hantsoo, L. V. Making Strides to Simplify Diagnosis of Premenstrual Dysphoric Disorder. *Am. J. Psychiatry* **174**, 6–7 (2017).
150. So, J., Warsh, J. J. & Li, P. P. Impaired Endoplasmic Reticulum Stress Response in B-Lymphoblasts From Patients With Bipolar-I Disorder. *Biol. Psychiatry* **62**, 141–147 (2007).
151. Hayashi, A. *et al.* Aberrant endoplasmic reticulum stress response in lymphoblastoid cells from patients with bipolar disorder. *Int. J. Neuropsychopharmacol.* **12**, 33–43 (2009).
152. Pfaffenseller, B. *et al.* Impaired endoplasmic reticulum stress response in bipolar disorder: cellular evidence of illness progression. *Int. J. Neuropsychopharmacol.* **17**, 1453–1463 (2014).
153. Van Wingen, G. A. *et al.* Progesterone selectively increases amygdala reactivity in women. *Mol. Psychiatry* **13**, 325 (2008).
154. Welihinda, A. A., Tirasophon, W. & Kaufman, R. J. The Cellular Response to Protein Misfolding in the Endoplasmic Reticulum. *Gene Expr.* **7**, 293–300 (2018).
155. Saito, A. & Imaizumi, K. Unfolded Protein Response-Dependent Communication and Contact among Endoplasmic Reticulum, Mitochondria, and Plasma Membrane. *Int. J. Mol. Sci.* **19**, (2018).
156. ZHU, G. & LEE, A. S. Role of the Unfolded Protein Response, GRP78 and GRP94 in Organ Homeostasis. *J. Cell. Physiol.* **230**, 1413–1420 (2015).
157. Carreras-Sureda, A., Pihán, P. & Hetz, C. Calcium signaling at the endoplasmic reticulum: fine-tuning stress responses. *Cell Calcium* **70**, 24–31 (2018).
158. Schwarz, D. S. & Blower, M. D. The endoplasmic reticulum: structure, function and response to cellular signaling. *Cell. Mol. Life Sci. CMLS* **73**, 79–94 (2016).
159. Timberlake, M. A. & Dwivedi, Y. Altered Expression of Endoplasmic Reticulum Stress Associated Genes in Hippocampus of Learned Helpless Rats: Relevance to Depression Pathophysiology. *Front. Pharmacol.* **6**, 319 (2015).

160. Bown, C., Wang, J. F., MacQueen, G. & Young, L. T. Increased temporal cortex ER stress proteins in depressed subjects who died by suicide. *Neuropsychopharmacol. Off. Publ. Am. Coll. Neuropsychopharmacol.* **22**, 327–332 (2000).

161. Uemura, T. *et al.* Bcl-2 SNP rs956572 associates with disrupted intracellular calcium homeostasis in bipolar I disorder. *Bipolar Disord.* **13**, 41–51 (2011).

162. Uemura, T., Green, M. & Warsh, J. J. CACNA1C SNP rs1006737 associates with bipolar I disorder independent of the Bcl-2 SNP rs956572 variant and its associated effect on intracellular calcium homeostasis. *World J. Biol. Psychiatry Off. J. World Fed. Soc. Biol. Psychiatry* **17**, 525–534 (2016).

163. Machado-Vieira, R. *et al.* The Bcl-2 gene polymorphism rs956572AA increases inositol 1,4,5-trisphosphate receptor-mediated endoplasmic reticulum calcium release in subjects with bipolar disorder. *Biol. Psychiatry* **69**, 344–352 (2011).

164. Perova, T., Wasserman, M. J., Li, P. P. & Warsh, J. J. Hyperactive intracellular calcium dynamics in B lymphoblasts from patients with bipolar I disorder. *Int. J. Neuropsychopharmacol.* **11**, 185–196 (2008).

165. Gold, P. W., Licinio, J. & Pavlatou, M. G. Pathological parainflammation and endoplasmic reticulum stress in depression: potential translational targets through the CNS insulin, klotho and PPAR-γ systems. *Mol. Psychiatry* **18**, 154–165 (2013).

166. Ii Timberlake, M. & Dwivedi, Y. Linking unfolded protein response to inflammation and depression: potential pathologic and therapeutic implications. *Mol. Psychiatry* (2018). doi:10.1038/s41380-018-0241-z

167. Levy, N. A. & Janicak, P. G. Calcium channel antagonists for the treatment of bipolar disorder. *Bipolar Disord.* **2**, 108–119 (2000).

168. Cipriani, A. *et al.* A systematic review of calcium channel antagonists in bipolar disorder and some considerations for their future development. *Mol. Psychiatry* **21**, 1324 (2016).

169. Thys-Jacobs, S., McMahon, D. & Bilezikian, J. P. Cyclical changes in calcium metabolism across the menstrual cycle in women with premenstrual dysphoric disorder. *J. Clin. Endocrinol. Metab.* **92**, 2952–2959 (2007).

170. Bocchieri, E. & Thys-Jacobs, S. Role of calcium metabolism in premenstrual syndrome. *Expert Rev. Endocrinol. Metab.* **3**, 645–655 (2008).

171. Quaranta, S., Buscaglia, M. A., Meroni, M. G., Colombo, E. & Cella, S. Pilot Study of the Efficacy and Safety of a Modified-Release Magnesium 250mg Tablet (Sincromag®) for the Treatment of Premenstrual Syndrome. *Clin. Drug Investig.* **27**, 51–58 (2007).

172. Popper, C. W. Do vitamins or minerals (apart from lithium) have mood-stabilizing effects? *J. Clin. Psychiatry* **62**, 933–933 (2001).
173. Carman, J., Post, R., Teplitz, T. & Goodwin, F. Divalent cations in predicting antidepressant response to lithium. *The Lancet* **304**, 1454 (1974).
174. Ascher, P. & Nowak, L. The role of divalent cations in the N-methyl-D-aspartate responses of mouse central neurones in culture. *J. Physiol.* **399**, 247–266 (1988).
175. Hiroi, T., Wei, H., Hough, C., Leeds, P. & Chuang, D.-M. Protracted lithium treatment protects against the ER stress elicited by thapsigargin in rat PC12 cells: roles of intracellular calcium, GRP78 and Bcl-2. *Pharmacogenomics J.* **5**, 102–111 (2005).
176. Nagy, T. *et al.* Lithium induces ER stress and N-glycan modification in galactose-grown Jurkat cells. *PloS One* **8**, e70410 (2013).

Figures

Figure 1. RNAseq analysis workflow

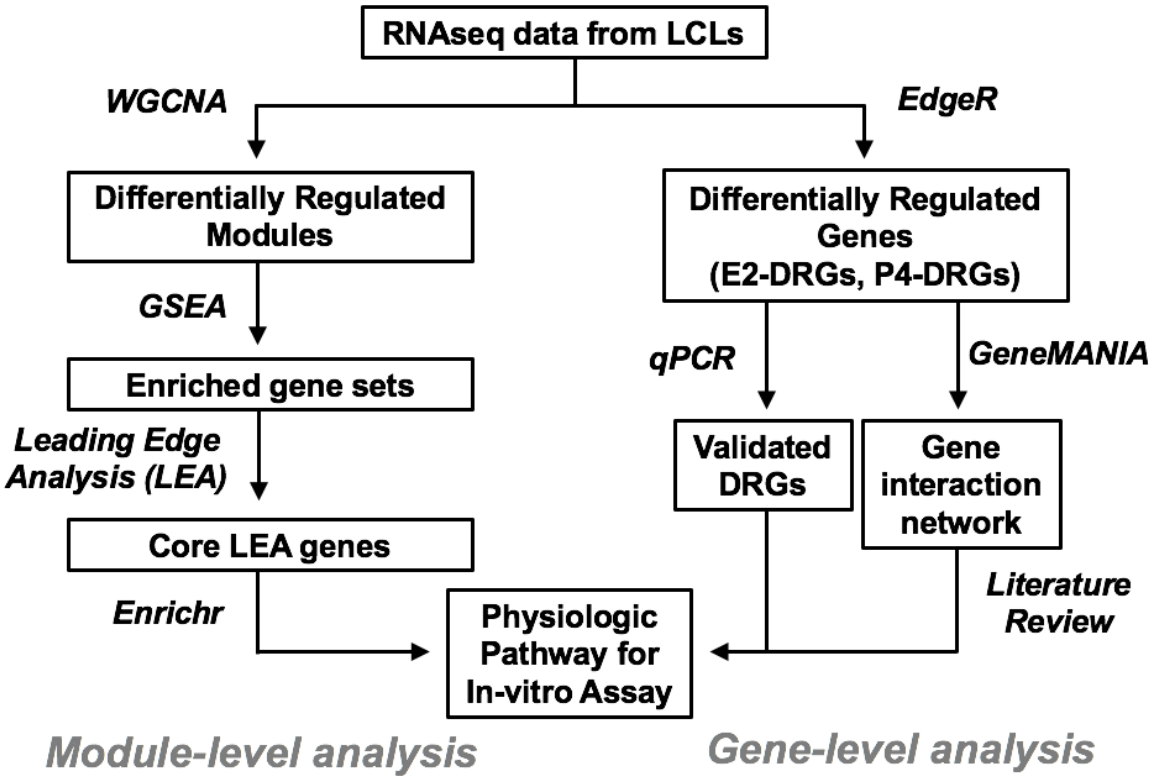

Figure 2. Functional analysis of WGCNA modules

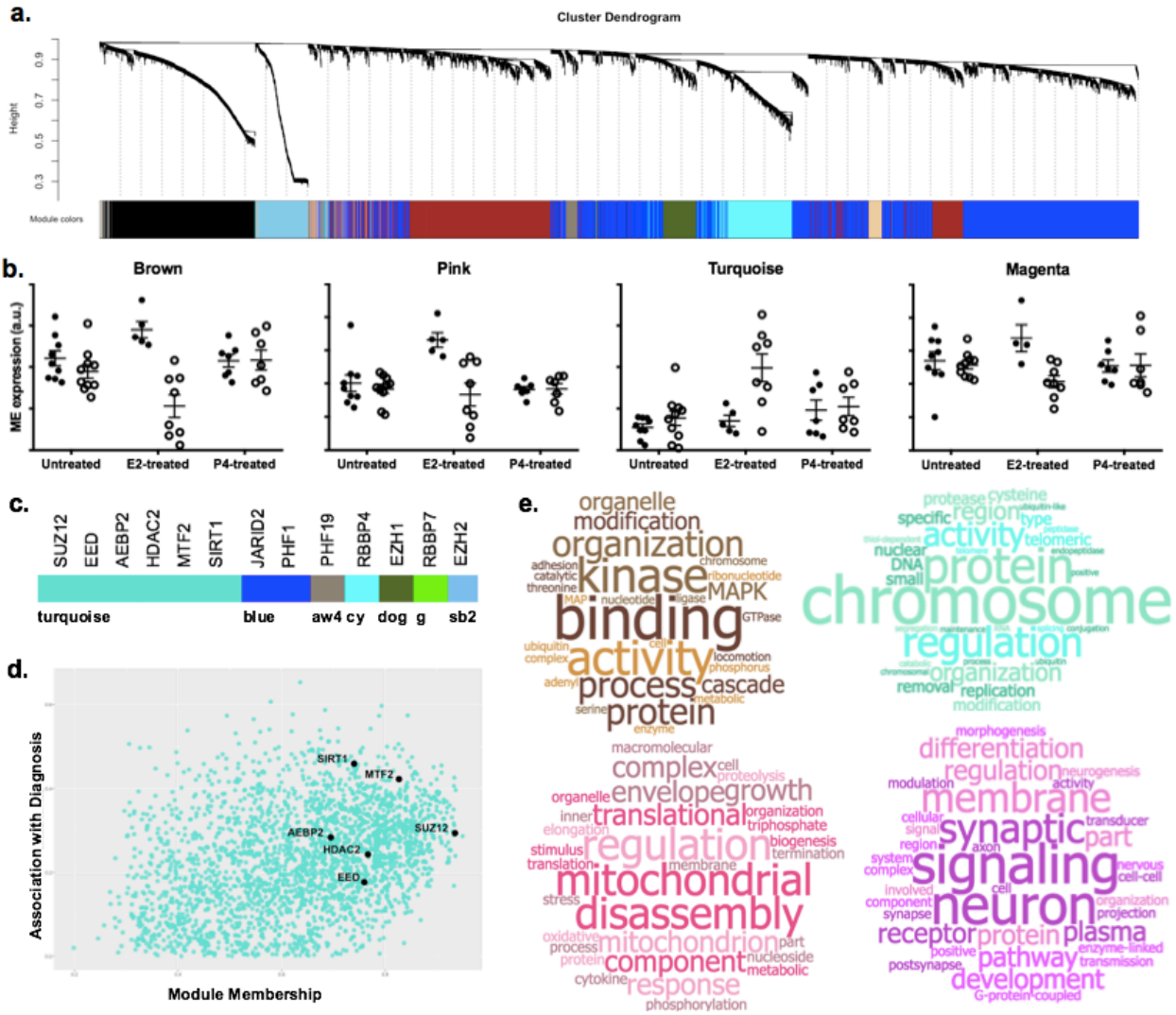

Figure 3. Enrichr analysis of magenta module LEA genes

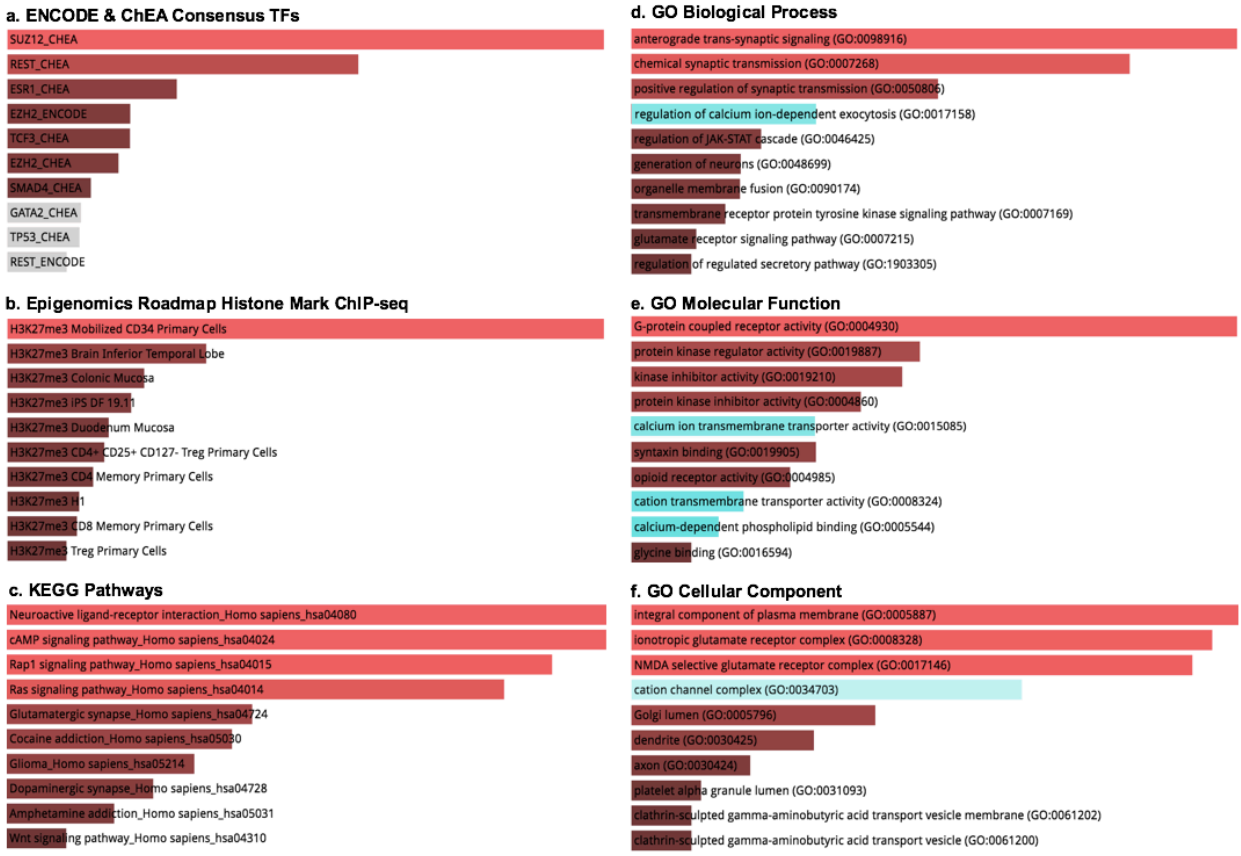

Figure 4. Network visualization and qPCR validation of Top E2-DRGs.

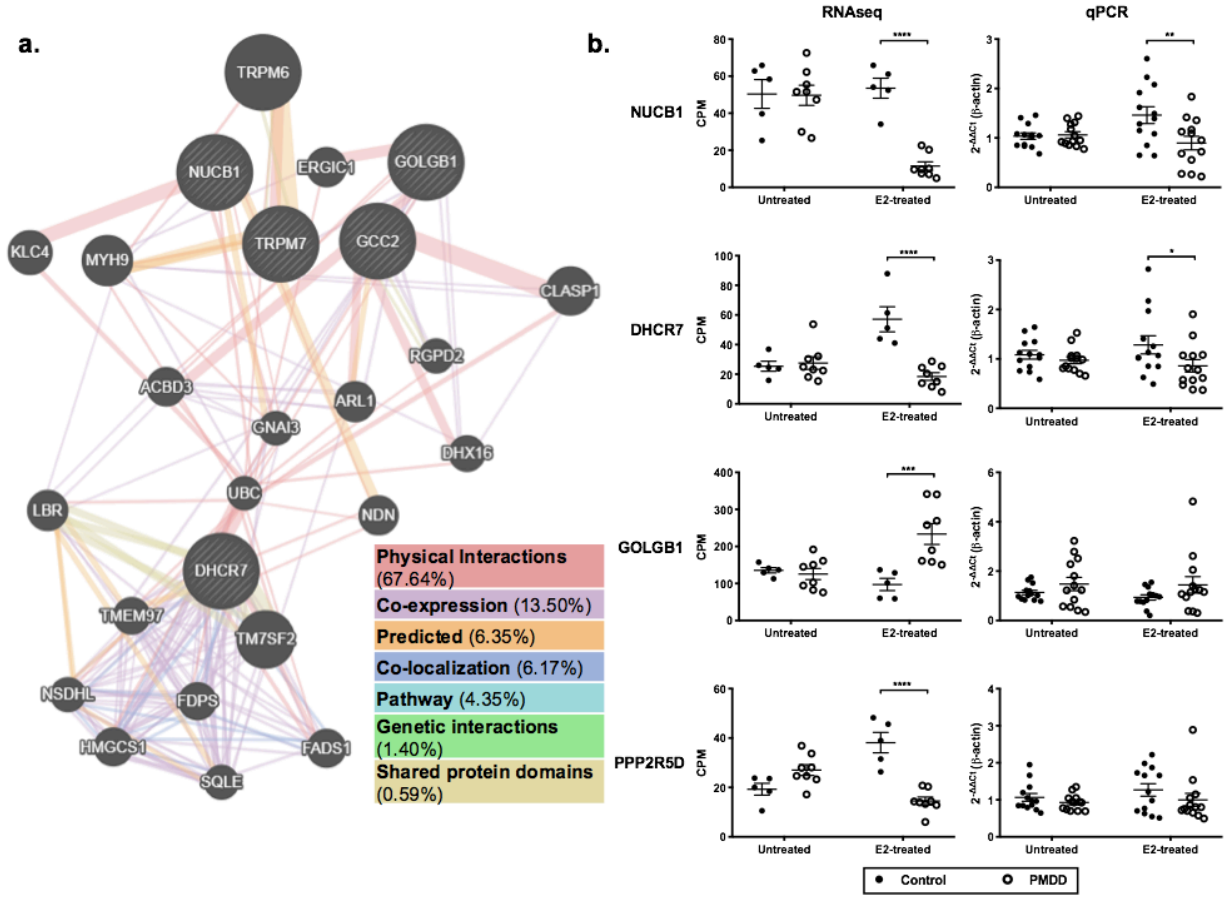

Figure 5. Thapsigargin challenge assays.

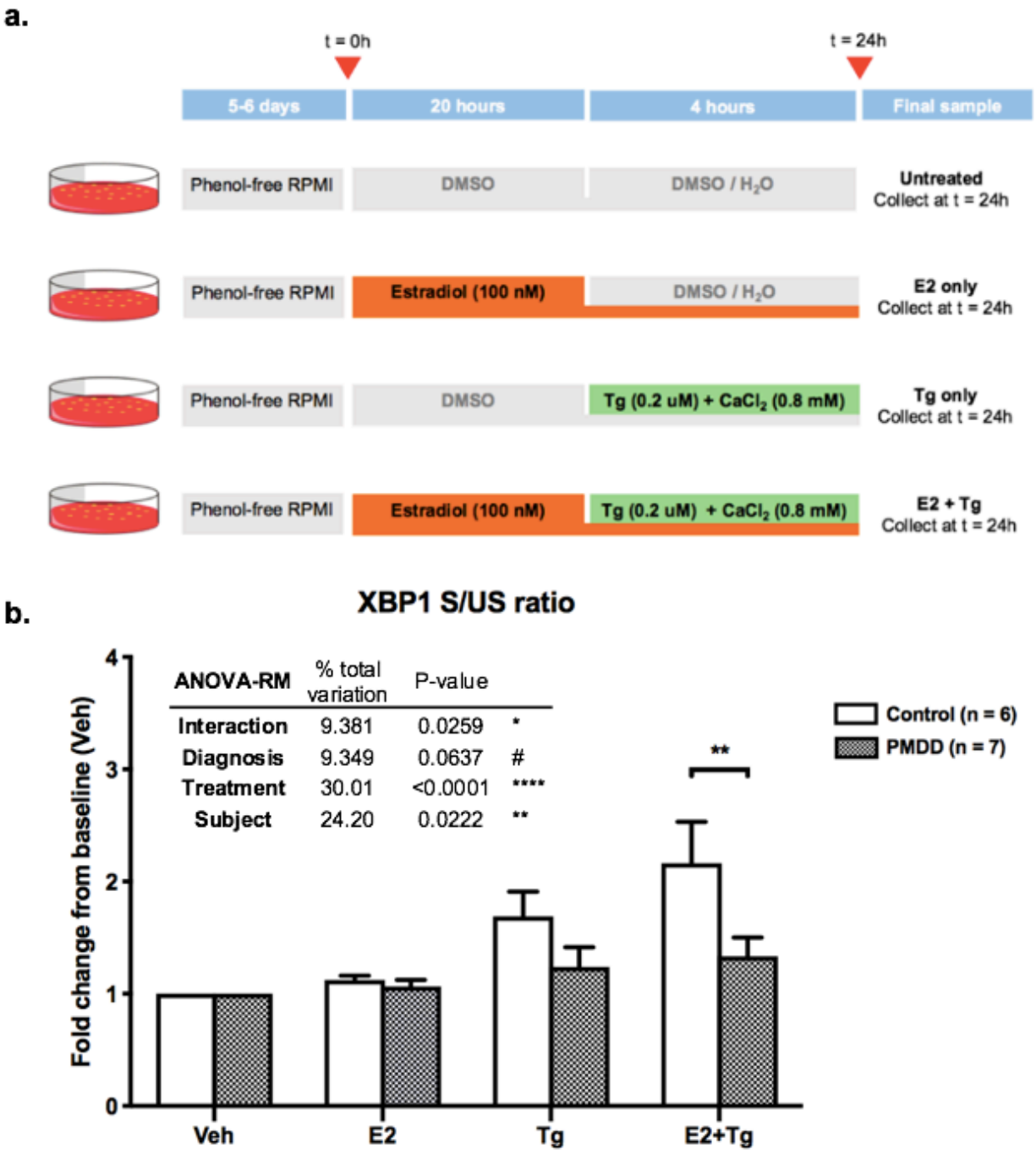

Supplemental Figures

Supplemental Figure S1. Response to E2, not P4 underlies the differential hormone response in PMDD

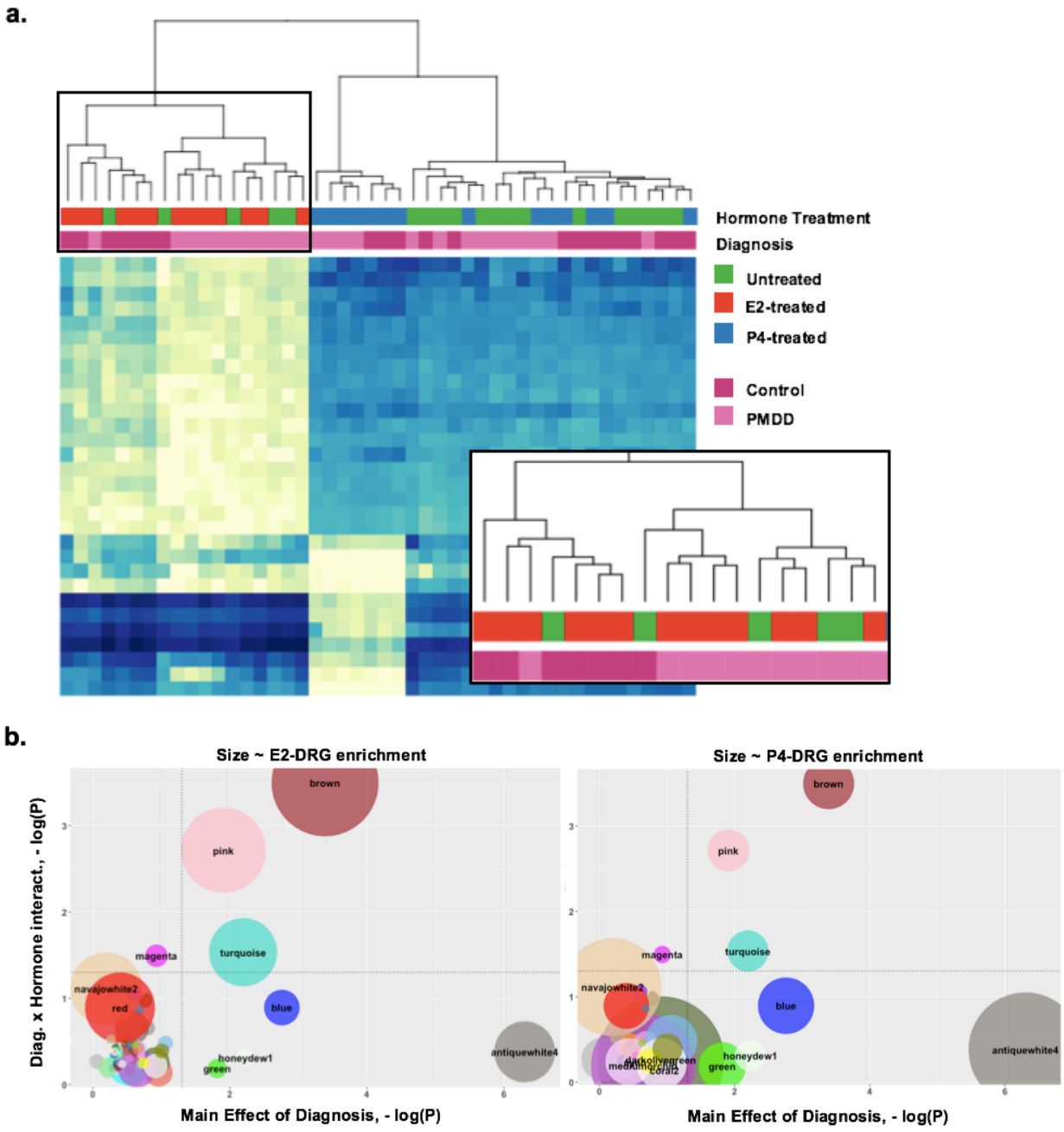

Tables

Table 1. Tabulated ANOVA P-values for effects of diagnoses and hormone treatment on module eigengene expression.

Module Eigengene	Two-way ANOVA Results (Pr > F)			Module Eigengene	Two-way ANOVA Results (Pr > F)		
	Diagnosis	Hormone Treatment	Interaction		Diagnosis	Hormone Treatment	Interaction
MEbrown	4.06E-04	3.50E-01	3.19E-04	MElightyellow	4.75E-01	1.92E-01	4.17E-01
MEpink	1.24E-02	6.83E-02	1.93E-03	MEsaddlebrown	2.60E-01	2.60E-01	4.19E-01
MEturquoise	6.37E-03	3.56E-03	2.92E-02	MEsienna3	3.30E-01	1.69E-01	4.24E-01
MEmagenta	1.17E-01	2.31E-01	3.21E-02	MEpalevioletred3	2.49E-01	4.10E-01	4.35E-01
MEnavajowhite2	6.40E-01	3.34E-02	7.75E-02	MEmediumpurple3	2.80E-01	5.23E-01	4.47E-01
MElightcyan	1.97E-01	4.24E-01	8.49E-02	MEdarkslateblue	4.88E-01	5.94E-01	4.48E-01
MEpurple	2.47E-01	3.05E-01	8.71E-02	MEplum1	1.96E-01	3.50E-01	4.56E-01
MEblack	1.72E-01	5.37E-01	1.05E-01	MEbrown4	2.22E-01	3.80E-01	4.59E-01
MEblue	1.73E-03	1.38E-05	1.28E-01	MEhoneydew1	5.85E-03	5.37E-01	4.88E-01
MEred	4.01E-01	8.89E-03	1.28E-01	MEviolet	2.91E-01	2.88E-01	4.92E-01
MEsteelblue	2.07E-01	4.71E-01	1.37E-01	MEdarkorange2	2.45E-01	5.35E-01	5.03E-01
MElightpink4	2.70E-01	5.06E-01	2.17E-01	MEgreenyellow	3.72E-01	2.38E-01	5.07E-01
MEgrey60	1.57E-01	1.15E-01	2.19E-01	MEgrey	8.82E-01	4.35E-01	5.41E-01
MEcoral1	4.02E-01	1.86E-01	2.87E-01	MEfloralwhite	3.90E-01	2.64E-01	5.45E-01
MEbisque4	3.43E-01	1.41E-01	2.89E-01	MEdarkolivegreen	1.24E-01	3.48E-05	5.51E-01
MEtan	5.47E-01	9.06E-02	2.97E-01	MEskyblue3	4.05E-01	2.65E-01	5.52E-01
MEdarkseagreen4	2.88E-01	1.48E-01	3.16E-01	MEyellow	1.81E-01	4.46E-01	5.61E-01
MElightcyan1	2.11E-01	3.67E-01	3.24E-01	MEmaroon	4.15E-01	3.92E-01	5.65E-01
MEskyblue2	8.67E-02	4.30E-03	3.30E-01	MEmidnightblue	4.40E-01	4.72E-01	5.73E-01
MEsalmon4	3.46E-01	1.73E-01	3.44E-01	MEthistle2	3.82E-01	3.21E-01	5.76E-01
MEdarkorange	2.33E-01	3.51E-01	3.45E-01	MEcyan	2.95E-01	7.34E-09	5.77E-01
MEyellowgreen	2.34E-01	3.12E-01	3.46E-01	MEthistle1	3.70E-01	3.47E-01	5.77E-01
MEplum2	2.06E-01	3.79E-01	3.54E-01	MEskyblue	1.94E-01	3.74E-01	5.80E-01
MEivory	3.71E-01	5.49E-01	3.55E-01	MEdarkred	1.75E-01	5.56E-01	6.02E-01
MElavenderblush3	2.32E-01	3.72E-01	3.65E-01	MEwhite	1.21E-01	2.85E-01	6.08E-01
MEdarkturquoise	3.19E-01	1.62E-01	3.71E-01	MEorangered4	4.31E-01	3.48E-01	6.32E-01
MEdarkgreen	4.54E-01	4.37E-01	3.72E-01	MElightgreen	5.87E-01	1.38E-01	6.37E-01
MEorange	3.41E-01	1.46E-01	3.73E-01	MEdarkmagenta	4.93E-01	4.25E-01	6.42E-01
MEpaleturquoise	1.90E-01	3.33E-01	3.80E-01	MEmediumorchid	2.26E-01	5.73E-02	6.43E-01
MEsalmon	2.16E-01	2.96E-01	3.82E-01	MEgreen	1.52E-02	1.78E-04	6.51E-01
MEroyalblue	3.17E-01	4.10E-01	3.89E-01	MEdarkgrey	2.90E-01	5.93E-01	6.77E-01
MEyellow4	9.85E-02	1.08E-02	4.06E-01	MElightsteelblue1	4.30E-01	3.13E-01	6.87E-01
MEantiquewhite4	4.97E-07	3.60E-02	4.16E-01	MEcoral2	1.09E-01	8.51E-01	7.25E-01

Table 2. Top 10 genes differentially regulated by estradiol in PMDD

Gene	Name	Summary	logCPM	F	P-Val
NUCB1	Nucleobindin 1	Member of a small calcium-binding EF-hand protein family. Thought to have a key role in Golgi calcium homeostasis and Ca(2+)-regulated signal transduction events.	5.31	28.99	4.28E-05
DST	Dystonin	Member of the plakin protein family of adhesion junction plaque proteins. Some isoforms expressed in neural and muscle tissue, anchoring neural intermediate filaments to the actin cytoskeleton.	8.52	24.13	1.17E-04
MDH2	Malate Dehydrogenase 2	Catalyzes the reversible oxidation of malate to oxaloacetate, utilizing the NAD/NADH cofactor system. Localized to the mitochondria.	7.49	23.07	1.48E-04
PPP2R5D	Protein Phosphatase 2 Regulatory Subunit B'Delta	Belongs to the phosphatase 2A regulatory subunit B family. One of the four major Ser/Thr phosphatases. Implicated in the negative control of cell growth and division. Cause of autosomal dominant intellectual disability.	4.61	22.27	1.78E-04
DHCR7	7-Dehydrocholesterol Reductase	Catalyzes the conversion of 7-dehydrocholesterol to cholesterol. Localizes to the ER membrane and nuclear outer membrane. Associated with Smith-Lemli-Opitz syndrome.	4.91	21.95	1.91E-04
GCC2	GRIP And Coiled-Coil Domain Containing 2	Peripheral membrane protein localized to the trans-Golgi network. Contains a GRIP domain thought to be used in Golgi targeting.	7.05	21.56	2.09E-04
GOLGB1	Golgin B1	May participate in forming intercisternal cross-bridges of the Golgi complex.	7.28	20.57	2.65E-04
GPI	Glucose-6-Phosphate Isomerase	Interconverts glucose-6-phosphate and fructose-6-phosphate in glycolysis. Extracellularly, functions as a neurotrophic factor that promotes survival of skeletal motor neurons and sensory neurons, and as a lymphokine that induces immunoglobulin secretion.	8.22	20.29	2.84E-04
PTP4A3	Protein-Tyrosine Phosphatase 4a3	A member of the protein-tyrosine phosphatase family. Enhances cell proliferation, motility, and promotes cancer metastasis. May be involved in the progression of cardiac hypertrophy by inhibiting intracellular calcium mobilization.	4.99	20.26	2.86E-04
SLC35A4	Solute Carrier 35A4	Probable UDP-sugar transporter protein. Paralog of SLC35A2, which transports UDP-galactose into Golgi vesicles, where it serves as a glycosyl donor for the generation of glycans.	5.20	19.87	3.15E-04

Supplemental Tables

Supplemental Table S1. Demographics of women contributing LCL cell lines for each study component

RNAseq experiments	**Controls (n = 9)**	**PMDD (n = 10)**	**P-value**
Race/Ethnicity	4 Caucasian 5 Black/African-American	6 Caucasian 4 Black/African-American	0.83
Age	36.9 (6.5)	40.6 (5.7)	0.21
BMI	27.8 (7.4)	27.2 (4.6)	0.85
Parity	1.2 (1.5)	1.7 (1.4)	0.48
Prior psychiatric history	0 Prior MDE 9 No prior hx	4 Prior MDE 5 No prior hx	0.10
Prior treatment history	0 Prior SSRI use 9 No prior tx	3 Prior SSRI use 7 No prior tx	0.25
qPCR validation	**Controls (n = 13)**	**PMDD (n = 13)**	**P-value**
Race/Ethnicity	10 Caucasian 2 Black/African-American 1 Asian	11 Caucasian 1 Black/African-American 1 Unknown	0.50
Age	29.6 (6.4)	38.9 (4.3)	**0.0003***
BMI	22.5 (3.6)	22.9 (2.4)	0.81
Parity	0.7 (1.2)	0.9 (1.2)	0.85
Prior psychiatric history	0 Prior MDE 13 No prior hx	1 Prior MDE 12 No prior hx	1
Prior treatment history	0 Prior SSRI use 13 No prior tx	1 Prior SSRI use 12 No prior tx	1
Tg challenge assays	**Controls (n = 6)**	**PMDD (n = 7)**	**P-value**
Race/Ethnicity	5 Caucasian 1 Black/African-American	2 Caucasian 5 Black/African-American	0.16
Age	36.2 (9.2)	37.0 (6.3)	0.86
BMI	26.4 (9.4)	28.9 (5.5)	0.60
Parity	1.8 (1.5)	1.3 (1.0)	0.46
Prior psychiatric history	0 Prior MDE 6 No prior hx	3 Prior MDE 4 No prior hx	0.24
Prior treatment history	0 Prior SSRI use 6 No prior tx	0 Prior SSRI use 7 No prior tx	1
Included in RNAseq?	4 Yes 2 No	5 Yes 2 No	1

Supplemental Table S2. Input RNAseq samples for WGCNA analysis

	Untreated	E2-treated	P4-treated	Total
Control	9	5	7	21
PMDD	10	8	7	25
Total	**19**	**13**	**14**	**46**

Supplemental Table S3. Top 20 GSEA results for Turquoise, Brown, Pink, and Magenta modules.

Turquoise					
GO Term	**Size**	**ES**	**NES**	**NOM p-val**	**FDR q-val**
Ubiquitin-like protein specific protease activity	34	0.53	2.82	0.00E+00	0.00E+00
Protein modification by small protein removal	35	0.52	2.73	0.00E+00	0.00E+00
Cysteine type endopeptidase activity	15	0.66	2.62	0.00E+00	0.00E+00
Thiol-dependent ubiquitin specific protease activity	25	0.56	2.61	0.00E+00	0.00E+00
Chromosome telomeric region	38	0.49	2.58	0.00E+00	0.00E+00
Cysteine type peptidase activity	40	0.48	2.58	0.00E+00	0.00E+00
Protein modification by small protein conjugation or removal	203	0.34	2.56	0.00E+00	2.86E-04
Protein catabolic process	133	0.35	2.49	0.00E+00	6.23E-04
Nuclear chromosome telomeric region	27	0.51	2.48	0.00E+00	6.66E-04
Chromosomal region	84	0.38	2.47	0.00E+00	6.00E-04
Positive regulation of chromosome organization	29	0.49	2.47	0.00E+00	6.35E-04
DNA replication	40	0.45	2.44	0.00E+00	8.30E-04
Chromosome	174	0.33	2.41	0.00E+00	1.23E-03
Regulation of DNA replication	31	0.47	2.39	0.00E+00	1.28E-03
Nuclear chromosome	81	0.36	2.34	0.00E+00	2.72E-03
Regulation of chromosome segregation	29	0.47	2.29	0.00E+00	5.17E-03
Chromosome organization	178	0.31	2.29	0.00E+00	4.92E-03
Regulation of chromosome organization	56	0.38	2.27	0.00E+00	5.59E-03
RNA splicing	73	0.35	2.25	0.00E+00	6.45E-03
Regulation of telomere maintenance	16	0.56	2.23	0.00E+00	7.82E-03

Brown					
GO Term	**Size**	**ES**	**NES**	**NOM p-val**	**FDR q-val**
Positive regulation of MAPK cascade	22	0.53	2.47	0.00E+00	1.68E-02
Regulation of MAPK cascade	31	0.46	2.44	0.00E+00	1.16E-02
Positive regulation of locomotion	15	0.59	2.42	0.00E+00	8.78E-03

GTPase binding	24	0.47	2.35	0.00E+00	1.24E-02
Enzyme binding	113	0.31	2.32	0.00E+00	1.33E-02
Positive regulation of protein modification process	56	0.35	2.21	1.07E-03	3.50E-02
Positive regulation of protein serine threonine kinase activity	16	0.53	2.18	1.28E-03	3.91E-02
Regulation of protein modification process	96	0.30	2.17	0.00E+00	3.76E-02
Positive regulation of phosphorus metabolic process	45	0.36	2.15	0.00E+00	4.03E-02
Kinase binding	39	0.37	2.07	1.14E-03	6.97E-02
Regulation of chromosome organization	16	0.50	2.07	3.82E-03	6.53E-02
Positive regulation of catalytic activity	84	0.29	2.05	1.04E-03	7.12E-02
Ubiquitin ligase complex	18	0.47	2.04	0.00E+00	7.23E-02
Positive regulation of organelle organization	37	0.36	2.04	1.15E-03	6.79E-02
Positive regulation of cell adhesion	18	0.47	2.00	6.44E-03	8.60E-02
Adenyl nucleotide binding	116	0.27	1.99	0.00E+00	8.46E-02
Regulation of organelle organization	77	0.29	1.98	2.09E-03	9.02E-02
Ribonucleotide binding	138	0.25	1.97	1.02E-03	8.96E-02
Regulation of MAP kinase activity	18	0.45	1.97	0.00E+00	8.58E-02
Positive regulation of kinase activity	21	0.43	1.96	1.25E-03	8.39E-02

Pink					
GO Term	**Size**	**ES**	**NES**	**NOM p-val**	**FDR q-val**
Mitochondrion organization	66	0.33	2.12	0.00E+00	3.13E-01
Translational elongation	22	0.43	2.00	3.71E-03	4.55E-01
Cellular response to stress	85	0.29	1.99	2.10E-03	3.50E-01
Organelle inner membrane	63	0.31	1.98	0.00E+00	2.76E-01
Regulation of cell growth	16	0.47	1.94	7.59E-03	3.13E-01
Mitochondrial envelope	77	0.29	1.92	1.05E-03	2.94E-01
Cellular protein complex disassembly	22	0.41	1.92	3.67E-03	2.63E-01
Cellular component disassembly	38	0.35	1.92	2.25E-03	2.35E-01
Envelope	92	0.27	1.89	2.07E-03	2.63E-01
Regulation of cellular component biogenesis	17	0.45	1.87	5.00E-03	2.62E-01
Translational termination	20	0.42	1.87	5.01E-03	2.38E-01
Macromolecular complex disassembly	24	0.40	1.87	1.06E-02	2.33E-01
Mitochondrial translation	21	0.41	1.86	2.36E-03	2.17E-01
Regulation of growth	20	0.42	1.85	1.21E-02	2.23E-01
Cellular response to cytokine stimulus	42	0.32	1.79	1.56E-02	3.18E-01
Nucleoside triphosphate metabolic process	32	0.34	1.78	1.03E-02	3.14E-01
Mitochondrial part	93	0.26	1.78	1.24E-02	3.05E-01
Mitochondrion	139	0.24	1.77	3.04E-03	3.17E-01

Proteolysis	43	0.31	1.76	1.77E-02	3.03E-01
Oxidative phosphorylation	18	0.40	1.76	1.53E-02	2.96E-01

Magenta					
GO Term	**Size**	**ES**	**NES**	**NOM p-val**	**FDR q-val**
Synaptic membrane	17	0.54	2.20	0.00E+00	1.00E-01
Neuron part	48	0.38	2.12	0.00E+00	1.03E-01
Cell-cell signaling	26	0.44	2.08	1.13E-03	9.67E-02
Neuron differentiation	20	0.47	2.08	1.19E-03	7.28E-02
Axon	15	0.51	1.98	5.07E-03	1.22E-01
Modulation of synaptic transmission	16	0.50	1.98	0.00E+00	1.08E-01
Postsynapse	18	0.46	1.95	2.45E-03	1.16E-01
Enzyme-linked receptor-protein signaling pathway	18	0.46	1.93	4.88E-03	1.14E-01
Synapse part	30	0.39	1.90	4.51E-03	1.36E-01
Neuron projection	39	0.36	1.89	7.61E-03	1.27E-01
Plasma membrane protein complex	19	0.45	1.89	7.16E-03	1.18E-01
Synaptic signaling	21	0.42	1.87	4.78E-03	1.21E-01
Regulation of nervous system development	31	0.37	1.86	6.72E-03	1.21E-01
Neuron development	16	0.47	1.86	7.39E-03	1.13E-01
Cell morphogenesis involved in differentiation	17	0.45	1.81	1.35E-02	1.50E-01
Signal transducer activity	34	0.35	1.80	6.63E-03	1.51E-01
Plasma membrane region	34	0.35	1.80	7.75E-03	1.49E-01
Positive regulation of cellular component organization	24	0.38	1.77	5.82E-03	1.63E-01
Neurogenesis	41	0.32	1.73	1.54E-02	2.03E-01
G protein-coupled receptor signaling pathway	27	0.36	1.72	1.57E-02	2.09E-01

Supplemental Table S4. Leading edge analysis of top 20 magenta module GSEA GO terms

		Gene set #																			
Gene	**Total**	**1**	**2**	**3**	**4**	**5**	**6**	**7**	**8**	**9**	**10**	**11**	**12**	**13**	**14**	**15**	**16**	**17**	**18**	**19**	**20**
OGFR	**2**	0	0	0	0	0	0	0	0	0	0	0	0	0	0	0	1	0	0	0	1
SNAP25	**11**	1	1	0	1	0	1	0	0	1	1	1	1	1	0	0	0	1	0	1	0
ACHE	**3**	0	0	0	1	0	1	0	0	0	0	0	1	0	0	0	0	0	0	0	0
ITGB4	**1**	0	0	0	0	0	0	0	0	0	0	1	0	0	0	0	0	0	0	0	0
C16orf45	**1**	0	0	0	0	0	0	0	0	0	0	0	0	0	0	0	0	0	0	1	0
SLC7A10	**2**	0	1	0	0	0	0	0	0	0	1	0	0	0	0	0	0	0	0	0	0
GRM3	**12**	1	1	0	1	1	1	1	0	1	1	0	1	0	0	0	1	1	0	0	1
CALB2	**3**	0	1	0	0	1	0	0	0	0	1	0	0	0	0	0	0	0	0	0	0
GPR173	**4**	0	0	0	0	0	0	0	0	0	0	0	0	1	0	0	1	0	0	1	1
RIMS4	**5**	1	1	0	0	0	1	0	0	1	0	0	0	0	0	0	0	1	0	0	0
HTR6	**4**	0	0	0	1	0	0	0	0	0	0	0	1	0	0	0	1	0	0	0	1
C8G	**1**	0	0	0	0	0	0	0	0	0	0	1	0	0	0	0	0	0	0	0	0
LRRTM3	**6**	1	0	0	0	0	0	1	0	1	0	0	0	1	0	0	0	1	1	0	0
LRRTM1	**10**	1	1	0	0	1	1	1	0	1	1	0	0	1	0	0	0	1	1	0	0
RAC3	**9**	0	1	1	1	0	0	0	0	0	1	0	1	1	1	0	0	0	1	1	0
HOXA2	**5**	0	0	1	0	0	0	0	0	0	0	0	0	1	1	1	0	0	0	1	0
SCN1A	**4**	0	1	0	0	1	0	0	0	0	1	1	0	0	0	0	0	0	0	0	0
IL11	**1**	0	0	0	1	0	0	0	0	0	0	0	0	0	0	0	0	0	0	0	0
TRPC6	**3**	0	0	1	0	0	0	0	0	0	0	0	0	1	0	0	0	0	0	1	0
ENTPD2	**1**	0	0	0	0	0	0	0	0	0	0	0	0	0	0	0	0	0	0	0	1
DSCAM	**7**	0	1	1	0	1	0	0	0	0	1	0	0	0	1	1	0	0	0	1	0
MMP2	**1**	0	0	0	0	0	0	0	1	0	0	0	0	0	0	0	0	0	0	0	0
ACTN1	**1**	0	0	0	0	0	0	0	0	0	0	0	0	0	0	1	0	0	0	0	0
OR2H1	**2**	0	0	0	0	0	0	0	0	0	0	0	0	0	0	0	1	0	0	0	1
TACR2	**2**	0	0	0	0	0	0	0	0	0	0	0	0	0	0	0	1	0	0	0	1
GPBAR1	**2**	0	0	0	0	0	0	0	0	0	0	0	0	0	0	0	1	0	0	0	1
GFRA1	**2**	0	0	0	0	0	0	0	1	0	0	0	0	0	0	0	1	0	0	0	0
ETV2	**1**	0	0	0	0	0	0	0	1	0	0	0	0	0	0	0	0	0	0	0	0
SRCIN1	**1**	0	0	0	0	0	0	0	0	0	0	0	0	0	0	1	0	0	0	0	0
F3	**1**	0	0	0	0	0	0	0	0	0	0	0	0	0	0	0	1	0	0	0	0
MAPK8IP1	**3**	0	1	0	0	1	0	0	0	0	1	0	0	0	0	0	0	0	0	0	0
CNKSR1	**1**	0	0	0	0	0	0	0	1	0	0	0	0	0	0	0	0	0	0	0	0
ZAP70	**2**	0	0	0	0	0	0	0	1	0	0	1	0	0	0	0	0	0	0	0	0
TMIGD2	**1**	0	0	0	0	0	0	0	0	0	0	0	0	0	0	0	1	0	0	0	0
C2CD4D	**2**	0	0	0	1	0	0	0	0	0	0	0	1	0	0	0	0	0	0	0	0
RGS7BP	**1**	0	0	0	0	0	0	0	0	0	0	0	0	0	0	0	0	0	0	0	1
ZFPM1	**1**	0	0	0	0	0	0	0	0	0	0	0	0	0	0	1	0	0	0	0	0
EPHA2	**7**	0	0	1	0	0	0	0	1	0	0	0	0	0	0	1	1	1	1	1	0
RNF165	**1**	0	0	0	0	0	0	0	0	0	0	0	0	0	0	1	0	0	0	0	0
CAMK2B	**8**	0	1	0	0	0	1	1	0	1	1	0	0	1	0	0	0	0	1	1	0
GNAZ	**3**	0	0	0	0	0	0	0	0	0	0	1	0	0	0	0	1	0	0	0	1
SDC3	**3**	0	1	0	0	1	0	0	0	0	1	0	0	0	0	0	0	0	0	0	0
ARX	**4**	0	0	1	0	0	0	0	0	0	0	0	0	0	1	1	0	0	0	1	0
OPRL1	**6**	0	1	0	1	0	0	0	0	0	1	0	1	0	0	0	1	0	0	0	1
GPR85	**2**	0	0	0	0	0	0	0	0	0	0	0	0	0	0	0	1	0	0	0	1
PDGFA	**2**	0	0	0	1	0	0	0	1	0	0	0	0	0	0	0	0	0	0	0	0
TGFA	**2**	0	0	0	0	0	0	0	0	0	0	0	0	0	0	0	0	1	1	0	0
SEMA3F	**5**	0	0	1	0	0	0	0	0	0	0	0	0	1	1	1	0	0	0	1	0
APCDD1	**1**	0	0	0	0	0	0	0	0	0	0	0	0	0	0	0	0	0	0	1	0
PRKCZ	**8**	0	1	1	0	1	1	0	1	0	1	0	0	0	1	0	0	0	0	1	0
AKAP3	**1**	0	0	0	0	0	0	0	1	0	0	0	0	0	0	0	0	0	0	0	0
GPR82	**2**	0	0	0	0	0	0	0	0	0	0	0	0	0	0	0	1	0	0	0	1
GNG3	**7**	0	1	0	0	0	0	1	0	1	1	1	0	0	0	0	1	0	0	0	1
GPR150	**2**	0	0	0	0	0	0	0	0	0	0	0	0	0	0	0	1	0	0	0	1
KISS1R	**3**	0	0	0	0	0	1	0	0	0	0	0	0	0	0	0	1	0	0	0	1
REPS2	**1**	0	0	0	0	0	0	0	1	0	0	0	0	0	0	0	0	0	0	0	0

NPTX1	**6**	0	0	1	1	0	0	0	0	0	0	0	1	0	1	1	0	0	0	1	0
HCRT	**7**	0	1	0	1	0	1	1	0	1	0	0	1	0	0	0	0	0	0	0	1
SCN3B	**2**	0	0	0	1	0	0	0	0	0	0	1	0	0	0	0	0	0	0	0	0
CACNG2	**2**	0	0	0	0	0	1	0	0	0	0	1	0	0	0	0	0	0	0	0	0
KCNJ1	**1**	0	0	0	0	0	0	0	0	0	0	1	0	0	0	0	0	0	0	0	0
TAS1R3	**2**	0	0	0	0	0	0	0	0	0	0	0	0	0	0	0	1	0	0	0	1
HES5	**4**	0	0	1	0	0	0	0	0	0	0	0	0	1	1	0	0	0	0	1	0
WNT3	**5**	0	0	1	0	0	0	0	0	0	0	0	0	0	1	1	1	0	0	1	0
SH2B2	**2**	0	0	0	0	0	0	0	1	0	0	0	0	0	0	0	1	0	0	0	0
LRRC4B	**8**	1	1	0	0	1	0	0	0	1	1	0	0	1	0	0	0	1	1	0	0
GDF11	**2**	0	0	0	0	0	0	0	1	0	0	0	0	0	0	0	0	0	0	1	0
SLC14A1	**1**	0	0	0	0	0	0	0	0	0	0	0	0	0	0	0	0	1	0	0	0
NMB	**4**	0	1	0	1	0	0	0	0	0	1	0	0	0	0	0	0	0	0	0	1
ZFHX3	**2**	0	0	0	0	0	0	0	0	0	0	0	0	1	0	0	0	0	0	1	0
SYT1	**12**	1	1	0	1	1	1	0	0	1	1	0	1	1	0	0	0	1	1	1	0
MAGEE1	**7**	1	1	0	0	0	0	1	0	1	1	1	0	0	0	0	0	1	0	0	0
FOXF2	**1**	0	0	0	0	0	0	0	0	0	0	0	0	0	0	1	0	0	0	0	0
NEGR1	**1**	0	0	0	0	0	0	0	0	0	0	0	0	0	0	0	0	0	0	1	0
CADM2	**3**	0	1	0	0	1	0	0	0	0	1	0	0	0	0	0	0	0	0	0	0
ATP2B2	**7**	0	1	1	0	0	1	0	0	0	0	0	0	0	1	1	0	1	0	1	0
SYT9	**4**	0	1	0	1	0	0	0	0	1	0	0	1	0	0	0	0	0	0	0	0
GRIN2B	**11**	1	1	0	1	0	0	1	1	1	1	1	1	0	0	0	1	1	0	0	0
RP1L1	**4**	0	1	1	0	0	0	0	0	0	0	0	0	0	1	0	0	0	0	1	0
NELL2	**2**	0	1	0	0	0	0	0	0	0	1	0	0	0	0	0	0	0	0	0	0
PTPRD	**2**	0	0	0	0	0	0	0	1	0	0	0	0	0	0	0	1	0	0	0	0
GRIN3B	**9**	1	1	0	1	0	0	1	0	1	0	1	1	0	0	0	1	1	0	0	0
MLPH	**2**	0	1	0	0	0	0	0	0	0	1	0	0	0	0	0	0	0	0	0	0
VANGL2	**1**	0	0	0	0	0	0	0	0	0	0	0	0	0	0	1	0	0	0	0	0
DPCR1	**1**	0	0	0	0	0	0	0	0	0	0	0	0	0	0	0	0	0	1	0	0
ID1	**6**	0	0	1	0	0	0	0	1	0	0	0	0	1	0	1	0	0	1	1	0
GJB5	**1**	0	0	0	0	0	0	0	0	0	0	1	0	0	0	0	0	0	0	0	0
PLP1	**5**	0	0	1	1	0	0	0	0	0	0	0	1	0	1	0	0	0	0	1	0

Supplemental Table S5. Enrichr analysis of Magenta LEA genes

ENCODE - ChEA Consensus TFs

Term	Overlap	Adjusted P-value	Z-score	Combined Score
SUZ12_CHEA	27/1684	1.03E-07	-1.54	31.16
REST_CHEA	18/1280	2.97E-04	-1.60	18.53
ESR1_CHEA	4/154	9.87E-02	-1.72	9.20
EZH2_ENCODE	5/338	2.08E-01	-1.66	6.81
TCF3_CHEA	10/1006	1.99E-01	-1.56	6.79
EZH2_CHEA	4/237	2.14E-01	-1.60	6.20
SMAD4_CHEA	6/584	3.69E-01	-1.53	4.78
GATA2_CHEA	7/772	3.69E-01	-1.46	4.26
TP53_CHEA	4/319	3.69E-01	-1.42	4.19
REST_ENCODE	4/383	5.50E-01	-1.46	3.53
POU5F1_CHEA	3/261	6.08E-01	-1.31	2.91
NANOG_CHEA	5/595	6.29E-01	-1.31	2.75
HDAC2_ENCODE	2/175	7.97E-01	-1.32	2.27
TP63_CHEA	9/1399	7.70E-01	-1.19	2.17
SALL4_CHEA	3/355	8.50E-01	-1.19	1.88
SOX2_CHEA	5/775	9.89E-01	-1.21	1.66
GATA1_CHEA	5/807	1.00E+00	-1.07	1.35
HNF4A_ENCODE	7/1276	1.00E+00	-1.12	1.25
BCL3_ENCODE	2/273	1.00E+00	-1.08	1.17
ZBTB7A_ENCODE	11/2184	1.00E+00	-0.97	0.98

Roadmap Epigenomics Histone Markers

Term	Overlap	Adjusted P-value	Z-score	Combined Score
H3K27me3 Mobilized CD34 Primary Cells	54/4453	1.10E-05	-1.74	29.80
H3K27me3 Brain Inferior Temporal Lobe	16/868	1.62E-02	-1.42	13.01
H3K27me3 Colonic Mucosa	27/3006	1.36E-01	-1.69	10.39
H3K27me3 iPS DF 19.11	26/2112	1.36E-01	-1.56	9.84
H3K27me3 Duodenum Mucosa	22/1866	1.50E-01	-1.52	8.90
H3K27me3 CD4+ CD25+ CD127- Treg Primary Cells	17/1199	1.36E-01	-1.42	8.71
H3K27me3 CD4 Memory Primary Cells	18/1574	1.53E-01	-1.45	8.24
H3K27me3 H1	39/4826	2.44E-01	-1.75	7.65
H3K27me3 CD8 Memory Primary Cells	19/1623	1.58E-01	-1.40	7.55
H3K27me3 Treg Primary Cells	13/856	1.58E-01	-1.31	7.11
H3K27me3 Duodenum Smooth Muscle	14/1054	2.00E-01	-1.40	7.06
H3K27me3 CD8 Naive Primary Cells	24/2258	2.44E-01	-1.48	7.03
H3K27me3 Rectal Smooth Muscle	18/1601	2.44E-01	-1.51	6.96
H3K27me3 H1 BMP4 Derived Trophoblast Cultured Cells	25/2683	2.44E-01	-1.50	6.72
H3K27me3 CD4+ CD25- CD45RA+ Naive Primary Cells	17/1476	2.44E-01	-1.34	5.91
H3K27me3 Stomach Smooth Muscle	12/993	2.44E-01	-1.31	5.80
H3K27me3 Breast vHMEC	15/1493	2.44E-01	-1.33	5.76
H3K4me1 CD4+ CD25- CD45RA+ Naive Primary Cells	28/3910	6.93E-01	-1.72	5.18
H3K27me3 CD4+ CD25int CD127+ Tmem Primary Cells	12/1106	4.02E-01	-1.27	4.76
H3K27me3 Stomach Mucosa	19/1479	4.63E-01	-1.33	4.72

KEGG Pathways

Term	Overlap	Adjusted P-value	Z-score	Combined Score
Neuroactive ligand-receptor interaction_Homo sapiens_hsa04080	7/277	1.23E-02	-1.89	15.94
cAMP signaling pathway_Homo sapiens_hsa04024	6/199	1.23E-02	-1.92	15.93
Rap1 signaling pathway_Homo sapiens_hsa04015	6/211	1.23E-02	-1.91	15.27
Ras signaling pathway_Homo sapiens_hsa04014	6/227	1.36E-02	-1.93	14.68
Glutamatergic synapse_Homo sapiens_hsa04724	4/114	2.94E-02	-1.80	11.58
Cocaine addiction_Homo sapiens_hsa05030	3/49	2.86E-02	-1.71	11.33
Glioma_Homo sapiens_hsa05214	3/65	3.90E-02	-1.87	10.87
Dopaminergic synapse_Homo sapiens_hsa04728	4/129	3.90E-02	-1.73	10.37
Amphetamine addiction_Homo sapiens_hsa05031	3/67	3.90E-02	-1.72	9.89

Wnt signaling pathway_Homo sapiens_hsa04310	4/142	3.90E-02	-1.65	9.30
Pathways in cancer_Homo sapiens_hsa05200	6/397	6.63E-02	-1.82	8.74
Arrhythmogenic right ventricular cardiomyopathy (ARVC)_Homo sapiens_hsa05412	3/74	4.22E-02	-1.48	8.05
Calcium signaling pathway_Homo sapiens_hsa04020	4/180	6.63E-02	-1.66	7.95
AGE-RAGE signaling pathway in diabetic complications_Homo sapiens_hsa04933	3/101	7.31E-02	-1.66	7.64
Circadian entrainment_Homo sapiens_hsa04713	3/95	6.63E-02	-1.57	7.46
Cholinergic synapse_Homo sapiens_hsa04725	3/111	8.11E-02	-1.60	6.97
Focal adhesion_Homo sapiens_hsa04510	4/202	8.11E-02	-1.54	6.81
Regulation of actin cytoskeleton_Homo sapiens_hsa04810	4/214	8.48E-02	-1.48	6.22
MAPK signaling pathway_Homo sapiens_hsa04010	4/255	1.19E-01	-1.41	5.15
Axon guidance_Homo sapiens_hsa04360	3/127	1.01E-01	-1.29	5.14

GO Biological Process

Term	Overlap	Adjusted P-value	Z-score	Combined Score
central nervous system myelination (GO:0022010)	2/9	3.53E-02	-2.97	21.69
megakaryocyte differentiation (GO:0030219)	2/10	3.53E-02	-2.99	21.16
anterograde trans-synaptic signaling (GO:0098916)	10/241	7.56E-05	-1.21	19.41
chemical synaptic transmission (GO:0007268)	10/290	2.09E-04	-1.35	19.39
neuron projection extension involved in neuron projection guidance (GO:1902284)	2/9	3.53E-02	-2.54	18.51
axon extension involved in axon guidance (GO:0048846)	2/9	3.53E-02	-2.52	18.41
sympathetic ganglion development (GO:0061549)	2/10	3.53E-02	-2.55	18.05
regulation of calcium ion-dependent exocytosis (GO:0017158)	4/54	1.67E-02	-1.84	17.03
semaphorin-plexin signaling pathway involved in neuron projection guidance (GO:1902285)	2/14	4.61E-02	-2.62	16.77
positive regulation of synaptic transmission (GO:0050806)	5/68	2.92E-03	-1.42	16.07
oligodendrocyte development (GO:0014003)	2/13	4.48E-02	-2.37	15.48
ganglion development (GO:0061548)	2/11	3.84E-02	-2.22	15.25
glutamate receptor signaling pathway (GO:0007215)	3/37	3.53E-02	-2.03	15.14
regulation of cell development (GO:0060284)	2/21	7.53E-02	-2.58	14.38
regulation of regulated secretory pathway (GO:1903305)	3/38	3.53E-02	-1.93	14.22
regulation of JAK-STAT cascade (GO:0046425)	4/66	2.91E-02	-1.62	13.73
transmembrane receptor protein tyrosine kinase signaling pathway (GO:0007169)	8/397	3.22E-02	-1.73	13.73
cardiac muscle cell contraction (GO:0086003)	2/18	6.42E-02	-2.25	13.24
sympathetic nervous system development (GO:0048485)	2/17	5.92E-02	-2.19	13.10
positive regulation of axon guidance (GO:1902669)	1/7	1.92E-01	-3.72	13.01

GO Molecular Function

Term	Overlap	Adjusted P-value	Z-score	Combined Score
opioid receptor activity (GO:0004985)	2/8	1.19E-02	-3.05	23.02
glycine binding (GO:0016594)	2/14	2.66E-02	-2.31	14.73
kinase inhibitor activity (GO:0019210)	4/60	7.45E-03	-1.51	13.43
cysteinyl leukotriene receptor activity (GO:0001631)	1/7	1.57E-01	-3.78	13.19
leukotriene receptor activity (GO:0004974)	1/7	1.57E-01	-3.77	13.17
syntaxin-1 binding (GO:0017075)	2/16	3.17E-02	-2.14	13.07
G-protein coupled receptor activity (GO:0004930)	9/268	4.37E-04	-1.02	13.06
calcium ion transmembrane transporter activity (GO:0015085)	4/78	1.03E-02	-1.66	13.00
protein kinase regulator activity (GO:0019887)	5/108	7.45E-03	-1.34	12.13
urea transmembrane transporter activity (GO:0015204)	1/7	1.57E-01	-3.26	11.39
voltage-gated ion channel activity involved in regulation of postsynaptic membrane potential (GO:1905030)	2/24	5.23E-02	-2.09	11.09
voltage-gated sodium channel activity (GO:0005248)	2/24	5.23E-02	-2.07	10.97
syntaxin binding (GO:0019905)	4/78	1.03E-02	-1.37	10.79
protein kinase inhibitor activity (GO:0004860)	4/68	9.08E-03	-1.25	10.49
vascular endothelial growth factor-activated receptor activity (GO:0005021)	1/8	1.57E-01	-2.97	9.98
calcium-dependent phospholipid binding (GO:0005544)	3/48	2.17E-02	-1.48	9.89

growth factor receptor binding (GO:0070851)	3/93	7.26E-02	-1.93	9.29
protein-hormone receptor activity (GO:0016500)	1/11	1.83E-01	-3.04	9.27
vinculin binding (GO:0017166)	1/11	1.83E-01	-2.94	8.95
cation channel activity (GO:0005261)	4/147	4.92E-02	-1.60	8.83
calcium channel activity (GO:0005262)	3/94	7.26E-02	-1.81	8.70

GO Cellular Component

Term	Overlap	Adjusted P-value	Z-score	Combined Score
NMDA selective glutamate receptor complex (GO:0017146)	2/10	1.52E-02	-2.71	19.15
ionotropic glutamate receptor complex (GO:0008328)	3/40	1.52E-02	-1.96	14.19
integral component of plasma membrane (GO:0005887)	16/1464	1.52E-02	-1.71	12.68
clathrin-sculpted gamma-aminobutyric acid transport vesicle membrane (GO:0061202)	1/9	2.10E-01	-3.23	10.48
clathrin-sculpted gamma-aminobutyric acid transport vesicle (GO:0061200)	1/9	2.10E-01	-3.18	10.33
pseudopodium (GO:0031143)	1/10	2.12E-01	-2.89	9.07
dendrite (GO:0030425)	4/216	1.37E-01	-2.06	8.63
cation channel complex (GO:0034703)	3/66	4.16E-02	-1.32	7.64
axon (GO:0030424)	3/142	1.91E-01	-2.02	7.48
T cell receptor complex (GO:0042101)	1/17	2.47E-01	-2.45	6.45
platelet alpha granule lumen (GO:0031093)	2/68	2.10E-01	-1.91	6.33
Golgi lumen (GO:0005796)	3/99	1.03E-01	-1.24	5.77
BLOC-1 complex (GO:0031083)	1/17	2.47E-01	-2.14	5.63
AMPA glutamate receptor complex (GO:0032281)	1/19	2.55E-01	-1.84	4.65
clathrin-coated vesicle membrane (GO:0030665)	2/82	2.28E-01	-1.45	4.34
platelet alpha granule (GO:0031091)	2/91	2.47E-01	-1.52	4.26
clathrin-coated vesicle (GO:0030136)	2/101	2.47E-01	-1.57	4.12
intrinsic component of mitochondrial inner membrane (GO:0031304)	1/30	3.72E-01	-1.68	3.51
mitochondrial intermembrane space (GO:0005758)	1/58	4.20E-01	-1.93	2.87
endoplasmic reticulum-Golgi intermediate compartment membrane (GO:0033116)	1/48	4.20E-01	-1.69	2.79

Supplemental Table S6. EdgeR output for significant E2-DRGs (top 100)

	logFC	logCPM	F	PValue	FDR
NUCB1	-2.235655847	5.313571982	28.98905842	4.28E-05	0.237502682
DST	1.339055855	8.516354707	24.12722694	0.000117056	0.237502682
MDH2	-1.527847426	7.486477428	23.06557398	0.000148211	0.237502682
PPP2R5D	-1.816748836	4.611969513	22.2721322	0.000177557	0.237502682
DHCR7	-1.708958861	4.911678136	21.95350483	0.000191121	0.237502682
GCC2	1.919680929	7.054028428	21.56080249	0.000209456	0.237502682
GOLGB1	1.445493056	7.279925121	20.56510631	0.000265393	0.237502682
GPI	-1.419602044	8.215311639	20.28870927	0.000283747	0.237502682
PTP4A3	-1.827483985	4.987282433	20.26148956	0.00028563	0.237502682
SLC35A4	-1.770559621	5.200674097	19.86670235	0.000314566	0.237502682
FNIP1	0.978184199	6.971968466	19.73995337	0.000324539	0.237502682
PPP1R14B	-1.319346671	5.493559485	19.39774369	0.000353274	0.237502682
RNPEP	-1.560563623	4.719050059	19.24732294	0.000366794	0.237502682
KMT2E	1.307053327	6.232164648	19.08103951	0.000382416	0.237502682
UFL1	1.294523804	6.170366828	18.44995257	0.000448842	0.237502682
ARID2	1.219588474	6.478719769	18.27686366	0.000469245	0.237502682
ALDOC	-1.237937743	7.573657855	18.21441391	0.000476859	0.237502682
TRAP1	-1.455243977	6.81452121	17.75930512	0.000536701	0.237502682
ILF3	-1.148177537	7.225137184	17.74243895	0.000539075	0.237502682
SIGMAR1	-2.756540494	3.16961827	17.5554733	0.000566186	0.237502682
MARCKSL1	-1.876358509	6.701510013	17.49717285	0.000574949	0.237502682
DUSP2	-1.920839983	7.651844957	17.4472633	0.000582571	0.237502682
HIVEP1	1.117336715	6.490006156	17.28256748	0.000608535	0.237502682
NACC1	-1.833900518	5.368672692	16.97209447	0.000661072	0.237502682
IDH2	-1.035772078	7.573361302	16.66816574	0.000717454	0.237502682
GRN	-1.915175998	6.919301143	16.62791126	0.000725317	0.237502682
MAP3K11	-1.901729384	4.414431834	16.25523336	0.000802863	0.237502682
DOPEY1	1.10480091	5.709822936	16.05560813	0.000848182	0.237502682
HIST1H2BC	-1.124225263	7.183626641	16.04069828	0.00085168	0.237502682
TNPO1	1.061005355	8.113722803	16.00453356	0.000860231	0.237502682
GUCD1	-1.397075697	6.191491057	15.76285484	0.000919903	0.237502682
BCKDHA	-1.812762804	5.736257613	15.70272388	0.00093546	0.237502682
USP34	1.124577629	8.397346442	15.68632922	0.000939752	0.237502682
RSF1	1.15216783	6.162019543	15.65118424	0.000949027	0.237502682
RBM25	1.137928547	6.280055517	15.63899573	0.000952268	0.237502682
BCKDK	-1.604865918	4.27118537	15.58318321	0.000967267	0.237502682
PYGO2	-1.303075811	4.687235035	15.51761827	0.000985224	0.237502682
NIPBL	1.052477096	7.959961126	15.43034726	0.001009707	0.237502682
TUFM	-1.375180393	6.254793304	15.40145631	0.001017962	0.237502682
RICTOR	0.986348253	7.139298912	15.25250021	0.001061735	0.237502682
ZNF37A	1.477277156	5.563157329	15.1337576	0.001098139	0.237502682
LINC00381	5.176531864	3.856666438	15.07410559	0.001116952	0.237502682
CWF19L2	1.129326504	5.303706491	15.06627713	0.001119448	0.237502682
ZNF507	1.284833237	5.703195359	15.06329607	0.0011204	0.237502682
CALML4	1.62155647	4.319773175	14.51913718	0.001310351	0.237502682
ASPM	1.734975782	6.527379034	14.45512456	0.001334972	0.237502682
STK25	-1.56576255	5.261374371	14.2898952	0.00140095	0.237502682
CEP83	1.89212416	5.231289117	14.28588704	0.001402595	0.237502682
QSER1	1.294343741	6.300561088	14.27999151	0.001405019	0.237502682
SCYL3	1.326138775	4.956382109	14.22775263	0.001426701	0.237502682
CD83	-1.498794337	5.197026375	14.21177777	0.001433406	0.237502682
ALYREF	-1.045283699	5.678312413	14.15860454	0.00145598	0.237502682
NRARP	-2.671108804	2.964190657	14.00451958	0.001523672	0.237502682
PIF1	-1.896586644	4.268313983	13.95903658	0.001544322	0.237502682
ZDBF2	1.297910049	6.848658205	13.90682444	0.001568413	0.237502682
PPP1R12A	0.968982205	7.4052167	13.85686678	0.001591858	0.237502682
MACF1	1.079850369	8.425805262	13.82961274	0.001604814	0.237502682
DMXL2	1.516360699	5.739932408	13.82200277	0.001608452	0.237502682
CHCHD10	-1.254528566	5.453577911	13.81262556	0.001612948	0.237502682

BIRC6	0.881147328	8.912757748	13.80283119	0.00161766	0.237502682
RPAP2	1.096269089	5.262447827	13.80130735	0.001618394	0.237502682
DNM1L	1.156606824	7.493378165	13.76018941	0.001638351	0.237502682
AFF1	0.952365931	7.657160009	13.7431569	0.001646699	0.237502682
SMARCD2	-1.142481684	5.839542074	13.66090859	0.001687684	0.237502682
TRIM26	-1.061390245	5.352422669	13.64128763	0.001697629	0.237502682
ZNF91	1.347314739	5.691921447	13.62943302	0.001703669	0.237502682
MPHOSPH9	1.115629929	6.436633982	13.61624325	0.001710418	0.237502682
ARL2	-2.005023223	4.251515998	13.61024596	0.001713497	0.237502682
WARS	-1.302362331	8.072687566	13.60515338	0.001716116	0.237502682
BCL2L1	-1.894298265	3.760659774	13.56441291	0.001737231	0.237502682
TJAP1	-2.338914658	3.43564346	13.40265831	0.00182398	0.237502682
HDGF	-0.999171812	6.678396428	13.3377848	0.001860125	0.237502682
SLTM	1.421751135	6.114481917	13.32200062	0.00186904	0.237502682
LRBA	0.970078818	8.580226625	13.24430478	0.001913628	0.237502682
THAP4	-1.878306554	4.55705865	13.20098626	0.001939003	0.237502682
NFKB2	-1.688366538	7.580048536	13.18869874	0.001946269	0.237502682
TAGLN2	-0.958398868	8.308641057	13.18121106	0.001950712	0.237502682
AKAP11	1.010394108	7.767251409	13.15983324	0.001963459	0.237502682
YTHDC2	1.097141205	6.121142851	13.12087941	0.001986927	0.237502682
SH2B1	-1.889647978	4.012811154	13.1157049	0.001990068	0.237502682
ERGIC2	1.087466814	5.785667146	13.02421213	0.002046533	0.237502682
FER	1.093156656	6.054029659	12.96730389	0.002082558	0.237502682
ELK4	1.078418314	7.26690713	12.95416421	0.002090976	0.237502682
ARSA	-2.214688981	3.805608515	12.92689032	0.002108572	0.237502682
ASF1B	-2.156972533	4.640988563	12.92156307	0.002112029	0.237502682
ZNF83	1.50463768	5.250085947	12.91615203	0.002115546	0.237502682
IP6K1	-1.609060994	4.77596863	12.90638156	0.002121913	0.237502682
SRM	-1.549503949	4.900112141	12.85006272	0.002159036	0.237502682
UTRN	1.185068756	6.740325603	12.84278685	0.002163885	0.237502682
RMI1	2.126389598	4.09696386	12.75753912	0.002221614	0.237502682
ZNF43	1.371866865	4.813435835	12.75482469	0.00222348	0.237502682
CXorf23	2.578437676	3.660726946	12.73817801	0.002234964	0.237502682
KIAA1109	1.130622163	7.231502499	12.67251853	0.002280912	0.237502682
PPP2R5E	1.288889379	6.555344376	12.57809499	0.002348855	0.237502682
SNORD38A	-2.093678377	5.856573384	12.57330927	0.002352358	0.237502682
RBM39	0.886007359	8.036533501	12.50687219	0.002401604	0.237502682
FHOD1	-1.71087721	4.473954088	12.47941867	0.00242229	0.237502682
U2AF1	-0.969175666	5.430603567	12.45485557	0.002440968	0.237502682
MYCBP2	0.873012544	8.294773561	12.41123175	0.002474537	0.237502682
FLAD1	-1.712931917	4.635498027	12.39050468	0.002490668	0.237502682

Supplemental Table S7. EdgeR output for significant P4-DRGs (top 100)

	logFC	logCPM	F	PValue	FDR
MAP3K3	0.921067899	4.543756545	19.49547251	0.000360031	0.935978106
SLC30A1	0.983126255	4.336646509	18.71358801	0.000437307	0.935978106
SNORD58A	1.5276668	7.922824937	17.91406135	0.000536043	0.935978106
SF3B2	0.677173959	6.923037187	17.63616306	0.000576021	0.935978106
VEGFB	1.111048997	4.976495467	17.36200907	0.000618756	0.935978106
LSS	0.93566208	5.792465124	16.85364157	0.000707727	0.935978106
COX5A	-1.111580055	6.101290037	16.54666061	0.000768346	0.935978106
PTPN7	-0.946001128	5.128410655	16.26980078	0.000828035	0.935978106
SNORD59A	0.985752428	5.663781719	15.44254974	0.001039694	0.935978106
TJP2	0.879539713	7.409520035	15.19053132	0.001115748	0.935978106
VBP1	-0.884636153	5.548187615	14.7909955	0.001249435	0.935978106
SNORD59B	1.289013152	5.394752718	14.38869998	0.001402448	0.935978106
GTPBP1	0.605005523	5.757099425	14.30889414	0.001435238	0.935978106
PRPF31	-0.938426263	4.55177528	14.16512981	0.001496496	0.935978106
GSG2	-1.413624116	3.032272318	13.70213479	0.001714608	0.935978106
YBX3	0.754385956	6.165574677	13.56731274	0.001784662	0.935978106
GMDS	-1.054204339	3.774515899	13.26878502	0.001951498	0.935978106
PXMP2	-1.910733392	2.824289583	13.21085734	0.001985859	0.935978106
SNORD58C	1.676841681	5.863830354	13.1052215	0.002050281	0.935978106
MARK4	1.054509511	3.785155939	12.97214775	0.002134797	0.935978106
FHL3	-1.396501382	2.671556952	12.82985406	0.002229521	0.935978106
ENO2	1.215849781	7.084211151	12.67226901	0.002339967	0.935978106
SNORD70	1.391306773	5.093804895	12.65074793	0.002355522	0.935978106
SNORD76	1.42687487	9.061353826	12.46826648	0.002492176	0.935978106
MEPCE	0.664508121	4.725685534	12.44868431	0.002507362	0.935978106
ZFAND3	0.88385961	5.070018921	12.3976986	0.00254739	0.935978106
ID3	-0.730887179	4.816969544	12.37289654	0.002567121	0.935978106
TCF20	0.587365184	6.475223747	12.36856637	0.002570584	0.935978106
SF1	0.742684219	6.282022922	12.28199214	0.002640919	0.935978106
ASS1	-2.055705963	2.914048807	12.15363693	0.00274921	0.941879236
NSMCE4A	-0.665609475	5.519053032	11.80894771	0.003065539	0.988814279
INSR	0.717738417	7.694601235	11.73143659	0.003142179	0.988814279
SNORA74B	-1.028962334	6.989011115	11.43919944	0.003451117	0.988814279
ZFP91	0.632507638	5.820869553	11.43207785	0.00345906	0.988814279
MARCKS	0.578995207	8.420324828	11.28424285	0.003628681	0.988814279
SNORA30	-1.251332358	5.222633087	11.28253847	0.00363069	0.988814279
GTF3C6	-1.037737709	4.436482053	11.21151451	0.003715542	0.988814279
SLC25A25	0.96852537	4.703060806	11.05708058	0.003907848	0.988814279
SNX17	-0.780361872	6.576622963	11.02181823	0.00395331	0.988814279
DNAJC5	0.800727608	5.241839908	10.95330466	0.004043353	0.988814279
CD38	-0.879348954	4.855510625	10.89523541	0.004121478	0.988814279
PPP2R5E	0.694875049	6.310263935	10.86350337	0.004164885	0.988814279
SNORD41	1.086202956	4.512812534	10.80644686	0.004244234	0.988814279
GTF2IRD1	1.385317417	3.927336977	10.80596256	0.004244915	0.988814279
SMARCA4	0.581115215	6.200733297	10.72496566	0.004360515	0.988814279
RELA	0.504769858	5.155138293	10.50253124	0.004696618	0.988814279
MCTP1	0.598925361	5.539395864	10.4783162	0.004734934	0.988814279
IL32	-1.06050273	8.138416786	10.43757335	0.004800199	0.988814279
RCOR1	0.881973563	4.547477394	10.34098919	0.004958996	0.988814279
EXOC8	0.630595669	4.976418161	10.0435429	0.00548642	0.988814279
SLC39A6	0.537702106	5.553549866	10.04180798	0.005489676	0.988814279
COCH	-0.845043138	4.168552384	10.03678601	0.005499113	0.988814279
RAB35	0.582933214	5.794887476	9.919235679	0.005725322	0.988814279
GOLGA2	0.578692143	5.363010796	9.900368275	0.005762597	0.988814279
CCNF	-0.81471133	4.207922942	9.884528685	0.005794101	0.988814279
GATAD2B	0.472528136	6.149261873	9.84727002	0.005868973	0.988814279
VNN2	-0.912718258	4.699392903	9.807645533	0.005949797	0.988814279
ACAA2	-0.540194562	6.799858743	9.789775108	0.005986658	0.988814279
P2RX5	-1.027862638	3.494693782	9.691489586	0.006194045	0.988814279

RNF10	0.509858529	6.684764203	9.665502438	0.006250223	0.988814279
USF2	0.984537879	6.993310696	9.658784301	0.006264839	0.988814279
CDK4	-0.526565698	6.477788085	9.546158628	0.006515697	0.988814279
GALNT10	0.640428553	6.478537204	9.494049042	0.006635578	0.988814279
TCF19	-0.88434514	4.802680541	9.468963953	0.006694173	0.988814279
ZBTB7A	0.852957283	4.251272788	9.459959771	0.006715347	0.988814279
MAGEF1	-1.177961409	3.131999414	9.443640279	0.006753917	0.988814279
USP42	0.631840027	5.012395071	9.395189995	0.006869903	0.988814279
PHF8	0.526122402	5.744159739	9.281613145	0.007150703	0.988814279
TGFB1	1.012900359	4.686566994	9.256455813	0.007214637	0.988814279
KAT8	0.678446489	4.086470802	9.245024993	0.007243899	0.988814279
TRIM21	-0.775115672	4.63361303	9.125454263	0.00755815	0.988814279
TRAK1	0.676468152	5.71767943	9.004624795	0.007891416	0.988814279
PECR	-0.6619727	4.333525185	8.994375107	0.00792044	0.988814279
PLXNA1	0.921598129	4.755778932	8.962842064	0.008010491	0.988814279
LAMP2	0.450390069	6.638047765	8.93612064	0.008087705	0.988814279
SPRYD3	1.122392161	3.210699711	8.935508176	0.008089485	0.988814279
YWHAQ	-0.727381537	7.332723833	8.924250844	0.008122273	0.988814279
SKIL	0.67652653	6.063541875	8.891771875	0.008217716	0.988814279
AIFM1	-0.665086196	5.692840217	8.849371959	0.008344222	0.988814279
C10orf12	0.766458455	3.853712604	8.838749966	0.008376258	0.988814279
SLC20A1	0.803261828	6.245840826	8.743888042	0.008668594	0.988814279
CMAHP	-0.827074073	4.324819188	8.709036654	0.008778874	0.988814279
RRP8	0.67622263	4.181038067	8.683030159	0.008862198	0.988814279
PSME1	-0.422673698	7.963515045	8.679617511	0.008873198	0.988814279
ETV3	0.869838143	3.515724273	8.547556419	0.009310954	0.988814279
DEXI	0.812904241	3.838644246	8.485524749	0.009524954	0.988814279
SETD1A	0.873941232	3.42440934	8.483004399	0.009533766	0.988814279
IFI44	-0.656082052	6.450138337	8.465687141	0.009594559	0.988814279
GIT1	0.728064649	4.329247283	8.441159345	0.009681416	0.988814279
HDAC7	-1.126989332	3.723216525	8.412308923	0.009784719	0.988814279
ARHGAP26	-0.491820038	4.950334019	8.408401691	0.009798805	0.988814279
IL2RB	0.609861214	6.694144664	8.335362275	0.01006638	0.988814279
TMOD1	-1.052531446	4.662809329	8.332344127	0.010077613	0.988814279
NFE2L2	0.482907291	6.130964366	8.310532933	0.010159213	0.988814279
HPS1	0.691666769	5.30008747	8.306715872	0.01017357	0.988814279
ARHGAP17	0.437692467	7.167650775	8.287989528	0.010244338	0.988814279
ADCY3	0.872839837	6.010197051	8.228876305	0.010471405	0.988814279
LPCAT4	1.014122617	3.940827739	8.200187431	0.010583651	0.988814279
IL7	0.712063319	3.988690983	8.140689613	0.010820799	0.988814279

Supplemental Table S8. ANOVA-RM Analysis of Tg challenge experiments.

Source of Variation	% of total variation	P value	
Interaction	9.381	0.0259	*
Diagnosis	9.349	0.0637	ns
Treatment	30.01	<0.0001	****
Subject	24.2	0.0222	*

ANOVA table	SS	DF	MS	F (DFn, DFd)	P value
Interaction	1.443	3	0.4809	F (3, 33) = 3.508	P=0.0259
Diagnosis	1.438	1	1.438	F (1, 11) = 4.250	P=0.0637
Treatment	4.615	3	1.538	F (3, 33) = 11.22	P<0.0001
Subject	3.721	11	0.3383	F (11, 33) = 2.468	P=0.0222
Residual	4.524	33	0.1371		

Post-hoc analysis: Within treatment, between group comparisons.

Sidak's multiple comparisons test	Predicted (LS) mean diff.	95.00% CI of diff.		Adjusted P Value
Controls - Cases				
Veh	0	-0.6254 to 0.6254	ns	>0.9999
E2	0.05635	-0.5691 to 0.6818	ns	0.9989
Tg	0.4493	-0.1762 to 1.075	ns	0.2481
E2+Tg	0.8286	0.2031 to 1.454	**	0.0051

Test details	Predicted (LS) mean 1	Predicted (LS) mean 2	Predicted (LS) mean diff.	SE of diff.	N1	N2	t	DF
Controls - Cases								
Veh	1	1	0	0.2408	6	6	0	44
E2	1.123	1.066	0.05635	0.2408	6	6	0.234	44
Tg	1.689	1.24	0.4493	0.2408	7	7	1.865	44
E2+Tg	2.162	1.334	0.8286	0.2408	7	7	3.44	44

Post-hoc analysis: Within group, between treatment comparisons.

Sidak's multiple comparisons test	Predicted (LS) mean diff.	95.00% CI of diff.		Adjusted P Value
Controls				
Veh vs. E2	-0.1226	-0.6602 to 0.4150	ns	0.9206
Veh vs. Tg	-0.6889	-1.227 to -0.1513	**	0.0085
Veh vs. E2+Tg	-1.162	-1.700 to -0.6247	****	<0.0001
Cases				
Veh vs. E2	-0.06626	-0.5640 to 0.4315	ns	0.9824
Veh vs. Tg	-0.2396	-0.7374 to 0.2581	ns	0.5515
Veh vs. E2+Tg	-0.3338	-0.8315 to 0.1640	ns	0.2738

Test details	Predicted (LS) mean 1	Predicted (LS) mean 2	Predicted (LS) mean diff.	SE of diff.	N1	N2	t	DF
Controls								
Veh vs. E2	1	1.123	-0.1226	0.2138	6	6	0.5735	33
Veh vs. Tg	1	1.689	-0.6889	0.2138	6	6	3.223	33
Veh vs. E2+Tg	1	2.162	-1.162	0.2138	6	6	5.437	33
Cases								
Veh vs. E2	1	1.066	-0.06626	0.1979	7	7	0.3348	33
Veh vs. Tg	1	1.24	-0.2396	0.1979	7	7	1.211	33
Veh vs. E2+Tg	1	1.334	-0.3338	0.1979	7	7	1.686	33